CTH–RF–72 May 1990

Measurements for the Energy Calibration of the TANSY Neutron Detectors

Krzysztof Drozdowicz *), Magnus Hök
and Dan Aronsson

CTH–RF–72 . May 1990

Measurements for the Energy Calibration of the TANSY Neutron Detectors

Krzysztof Drozdowicz *), Magnus Hök
and Dan Aronsson

*) *permanent address*
The Henryk Niewodniczański Institute of Nuclear Physics
ul. Radzikowskiego 152, PL–31–342 Kraków, Poland

Department of Reactor Physics
Chalmers University of Technology, S–412 96 Göteborg
ISSN 0281–9775

CTH–RF–72

MEASUREMENTS FOR THE ENERGY CALIBRATION OF THE TANSY NEUTRON DETECTORS

K. Drozdowicz, M. Hök, and D. Aronsson

Abstract

The report describes measurements performed for the energy calibration of the TANSY neutron detectors (two arrays of 16 detectors each one). The calibration procedure determines four calibration parameters for each detector. Results of the calibration measurements are given and test measurements are presented. A relation of the neutron detector calibration parameters to producer's data for the photomultipliers is analysed. Also the tests necessary during normal operation of the TANSY neutron spectrometer are elaborated (passive and active tests). A method how to quickly get the calibration parameters for a spare detector in an array of the neutron detectors is included.

Contents

1. Introduction

This report presents measurements performed for the calibration of the TANSY neutron detectors. It is also thought as a part of the documentation of the TANSY spectrometer and therefore contains a number of quite detailed data.

A method for the energy calibration of the neutron detectors has been presented in ref.[1]. The TANSY spectrometer [2] [3] contains two arrays of 16 neutron detectors each, which are here called branches A and B. An energy calibration should give a dependence of the amplitude of the fast output signal on incoming radiation energy. A γ source is used for the calibration of the neutron detectors. Because of a different interaction mechanism in the scintillator in the two cases, all energies are referred to the electron energy. For details see ref.[1].

The amplitude of the output signal, A, is given by Eq.(19a) in [1] as a function of the incoming energy, E, and the high voltage, V, applied to the photomultiplier:

$$\ln(A) = K_0 + n \cdot \ln(V) + \ln(E/E_0) \ , \tag{1}$$

where

E_0 is the energy of the calibration γ source (referred to the electron energy scale, *cf* Fig.11 in [1]),

K_0 is a constant (dependent on the E_0 energy, the sensitivity of the detector, and a coefficient in amplification in the photomultiplier tube and base), and

n is a constant proportional to the number of dynodes in the photomultiplier.

When the calibration γ source is used, Eq.(1) gives for the i^{th} neutron detector:

$$\ln(A_i) = K_{0i} + n_i \cdot \ln(V) \ , \tag{2}$$

where K_{0i} and n_i are called the calibration parameters of the i^{th} detector and are to be found. In the electronic system (see Fig.2 in [1]) the lower (LL) and upper (UL) level discriminators are used. The signal for the UL discriminator is attenuated (by a factor of approximately two, varying between channels) and therefore the i^{th} neutron detector is described by a set of four calibration parameters, K_{0Li}, n_{Li}, K_{0Ui}, n_{Ui}.

An important constant which is used in the calculation of the settings for the neutron detectors (discrimination levels and high voltages) is the energy E_0, *ie* the energy corresponding to the peak position of the amplitude distribution of the calibration source, when the Compton energy, E_C, of this γ source is defined at the half–peak position (see Fig.11 in [1]). The energy E_0 for the ^{60}Co source used in the calibration procedure has been determined experimentally.

2. Determination of the Calibration Parameters

2.1. Method of the Measurement

The neutron detector calibration parameters, $\{K_{0L}, n_L, K_{0U}, n_U\}_{i=0,...,15}$, for branches A and B of the spectrometer are measured with the method described in paragraph 3.3 in [1]. The count rate measurement is done, *ie* the number of counts P as a function of the detector high voltage V is recorded. This is done at a certain discrimination level D_j for all 16 detectors at the same time. Peak positions V_j in the differential distributions dP/dV give points $(V_j, D_j)_{i=0,...,15}$ on the line described by Eq.(2) (in the measurement the amplitude equal to the discrimination level, $A_j = D_j$, is detected). A change of the discrimination level gives another series of the points $(V_{j+1}, D_{j+1})_i$, see Fig.7 in [1]. Finally, the experimental straight lines, Eq.(2), are obtained for all detectors. A fit gives the required calibration parameters.

A linear dependence D(V) is limited to a certain range of the amplitudes. During elaboration of the method of the energy calibration of the neutron detectors, measurements were performed in a wide range of discrimination levels to find a proper interval of a linear dependence in the investigated system. A typical example is given in Fig.1, where a saturation effect is observed. At at a very low discrimination level non–linearity appears due to high fluctuations of the discrimination and DC levels (although only of order of millivolts). From such measurements intervals of the discrimination levels were chosen according to: $100\,mV < D_L < 1000\,mV$ and $D_U < 1000\,mV$. Here D_L and D_U are the discrimination levels of the lower and upper discriminators, respectively. One has to remember that the input signal to the UL discriminator is attenuated about 50 per cent. During the measurements of the calibration parameters K_{0U} and n_U the UL discriminator is used in the role of a single, lower level discriminator.

A series of computer programs has been created to control the measurements, to collect and rearrange experimental data, to elaborate them, and to get the final result – neutron detector calibration parameters and the required settings of discriminators and high voltages for the detectors. The full calibration procedure using these programs is illustrated in Fig.2. An essential part of the program [4] for remote control of the high voltage unit is included in the program HVCAL which also controls the CAMAC scalers and sorts the data. The system has been controlled by the CES "STARBURST" computer, RSX–11M operation system.

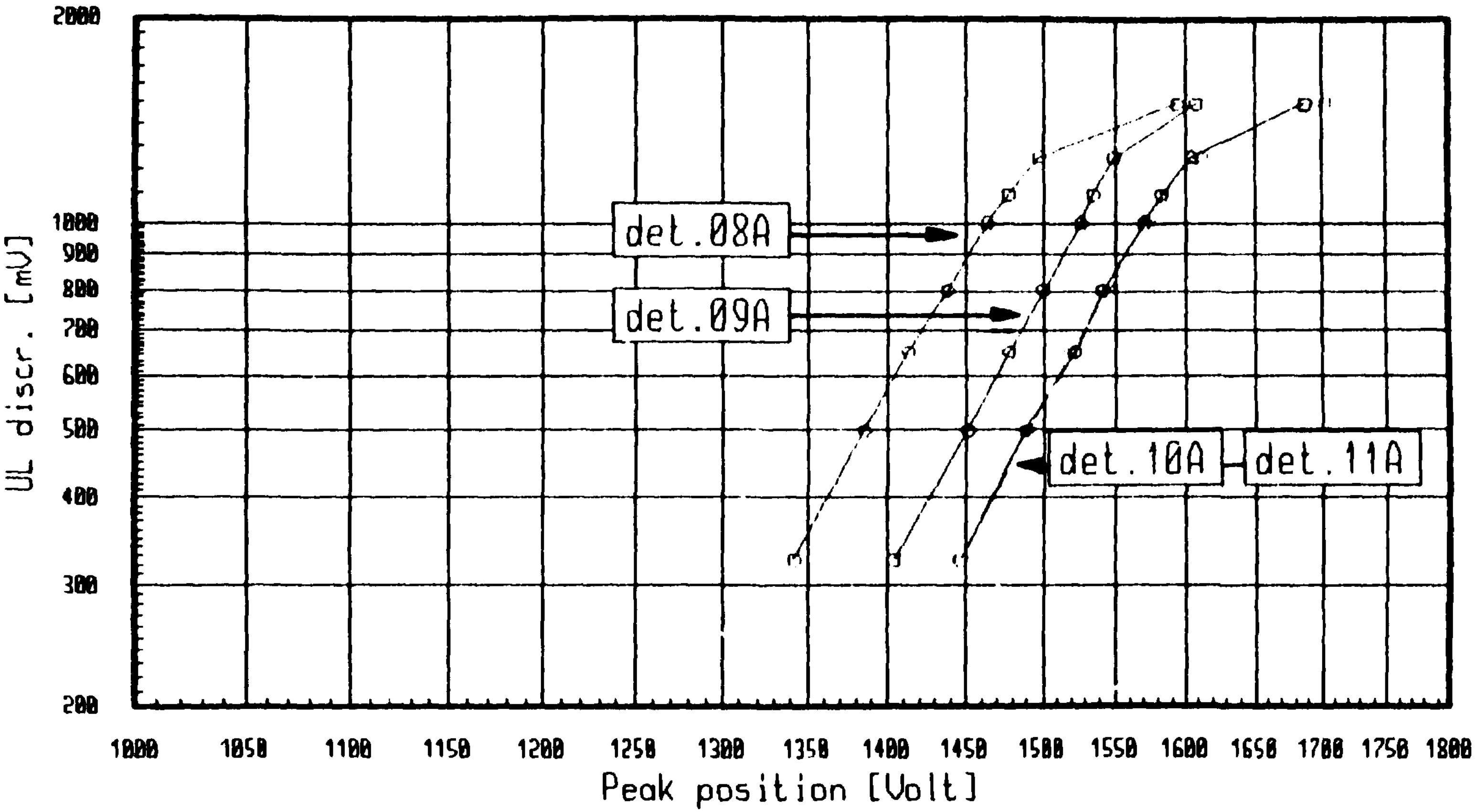

Fig.1. Saturation effect of the pulse amplitude at a high PM gain.

1. Preset discrimination levels for all detectors.

2. (Run a test for the count rate measurement)*T

3. Run the count rate distribution measurement (all the detectors simultaneously)

4. Get the differentiated distributions, observe the results.

5. Get the positions of the maxima $(V_{Pj})_i$ of the differentiated distribution.

6. Repeat steps 1 – 5 several times, for different discriminator levels

(continued)

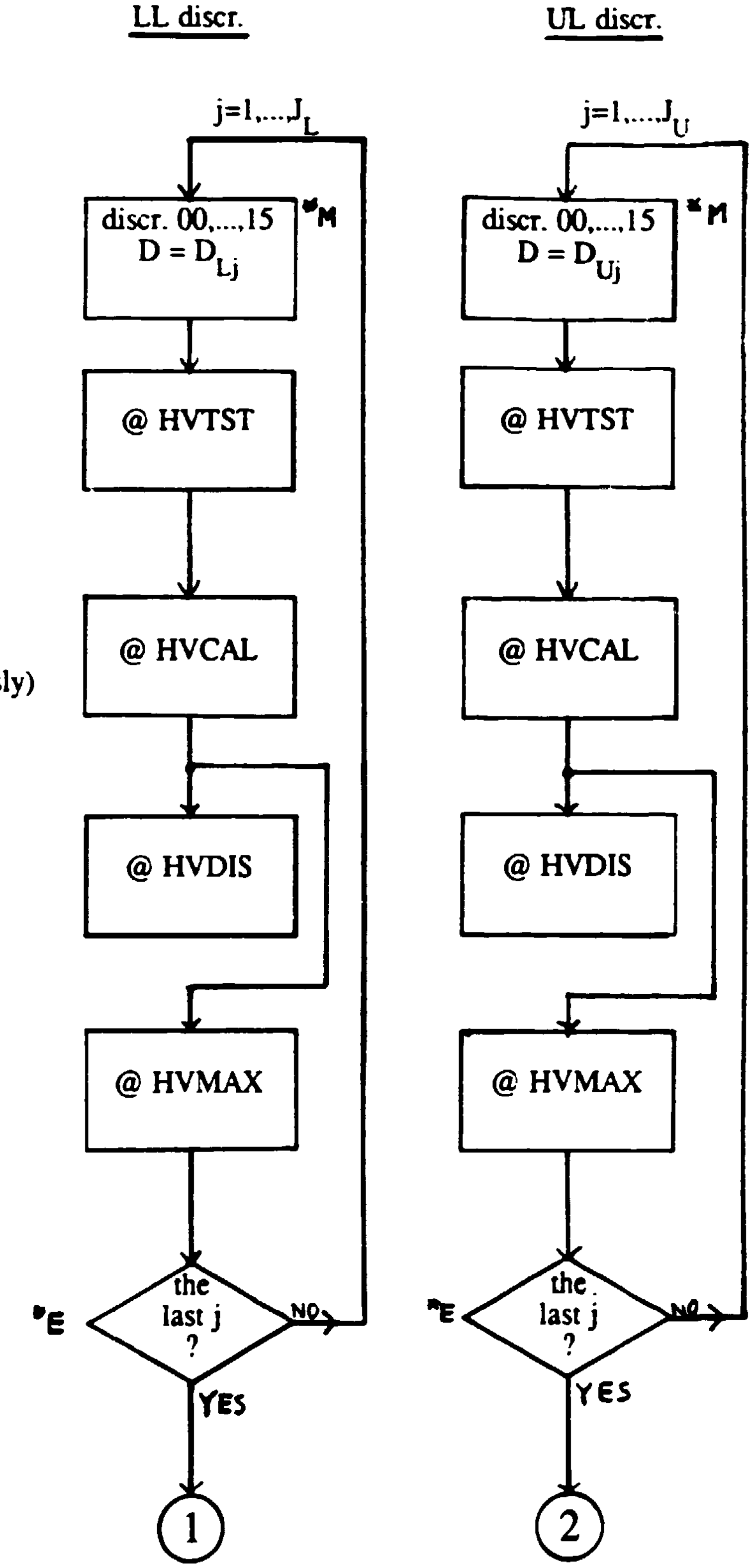

7. Rearrange the result data files

8. Plot the results for each detector

9. Get the neutron detector calibration paramaters $\{K_{0i}, n_i\}$

10. Create the full complet of the neutron detector parameters $\{K_{0L}, n_L, K_{0U}, n_U\}_{i=0,...,15}$

11. Get neutron detector settings $\{V_i, D_{Ui}\}$ at required conditions: D_L, E_L, E_U

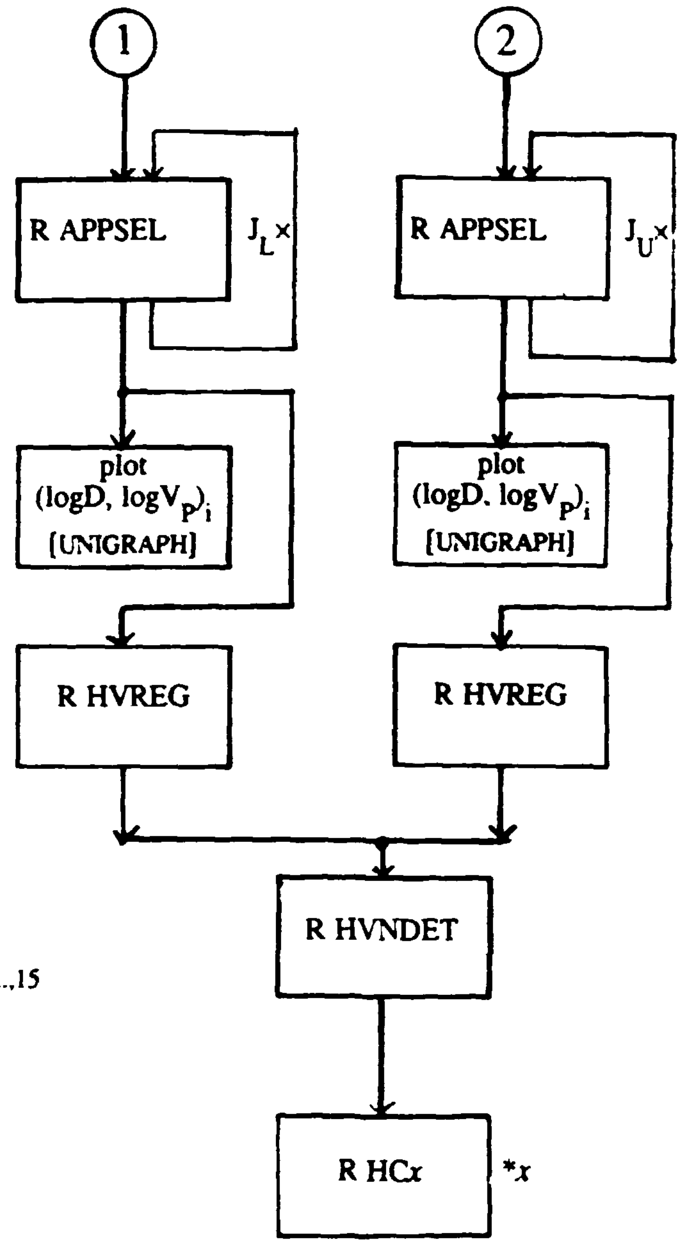

Fig.2. Scheme of the calibration procedure of the neutron detectors.

Symbols: R – run a single computer task, @ – run a series of tasks.

*E) experimenter's decision

*M) manually

*T) before the first measurement and later if necessary

*x) R HCA for branch A and R HCB for branch B, the data files are rigorously separated to avoid any serious mistake.

2.2. Results of the Measurements

The count rate integral distribution measurements were performed for both the branches, A and B, at the following discrimination levels:

LL: D_L = 100, 150, 250, 400, 600, 900 mV

UL: D_U = 300, 400, 500, 650, 800, 1000 mV (attenuated input signal) .

The curves were differentiated and the peak positions V_{Pj} were found. A typical result is shown in Fig.3 (branch A, D_L = 150 mV).

The results of the $(D_j, V_{Pj})_i$ measurements for all detectors are plotted in Figs 4–7. Four detectors are presented in each plot. The scale is kept the same all the time to make a visual comparison feasible. There are plotted lines connecting points and not fit–lines for a better presentation in some cases of almost overlapping points. Very big differences in sensitivity of the detectors are observed as significant shifts of the plotted lines but they are almost parallel. (The slope is given by n_i , which is a constant proportional to the number of dynodes of the photomultiplier and it should be the same for each detector in the ideal case of full reproducibility manufacturing the photomultipliers).

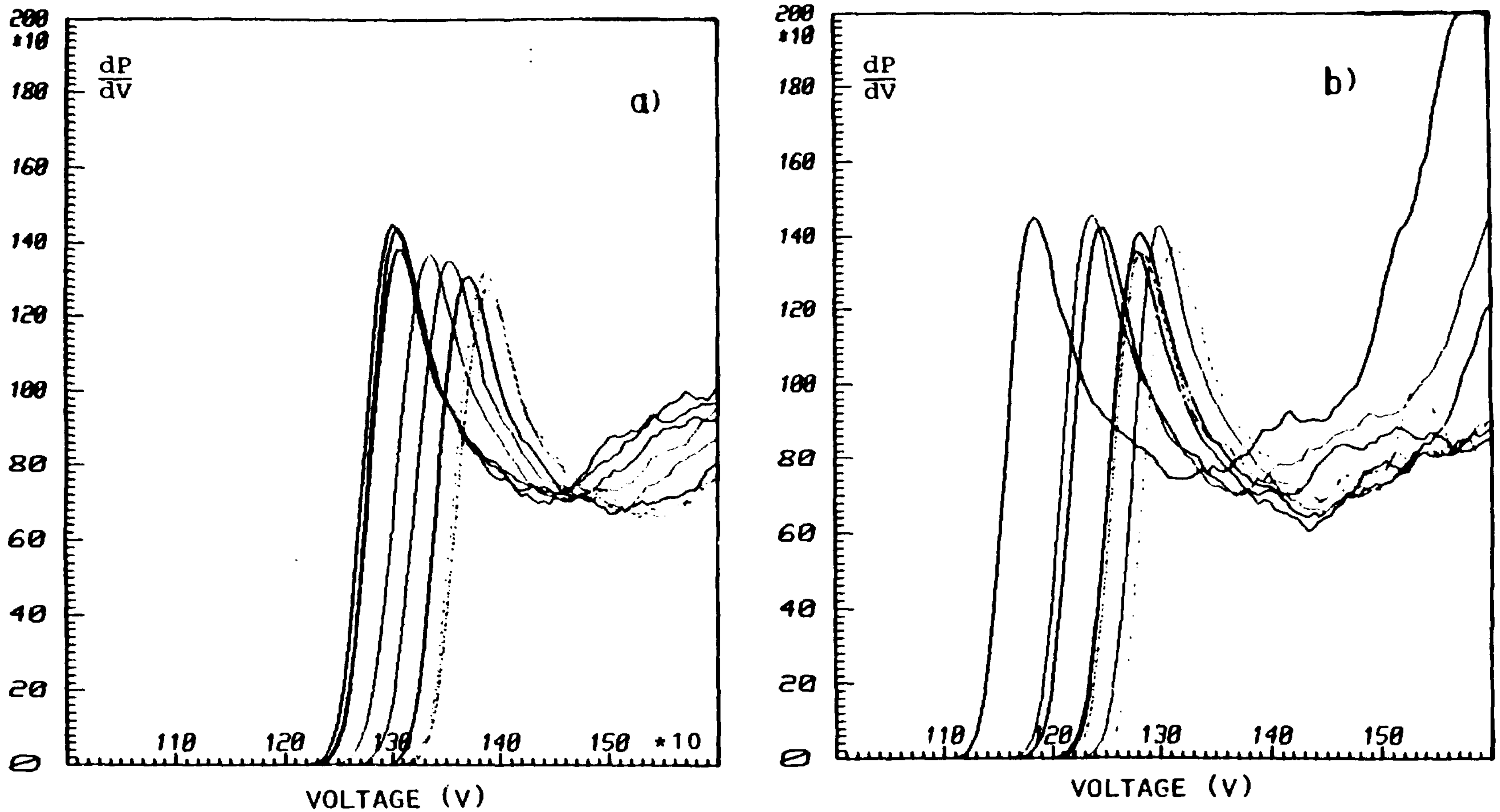

Fig.3. Typical differential countrate distributions, dP/dV = f(V). Branch A, LL discriminators: D_L = 150 mV. a) detectors 00A – 07A, b) detectors 08A – 15A.

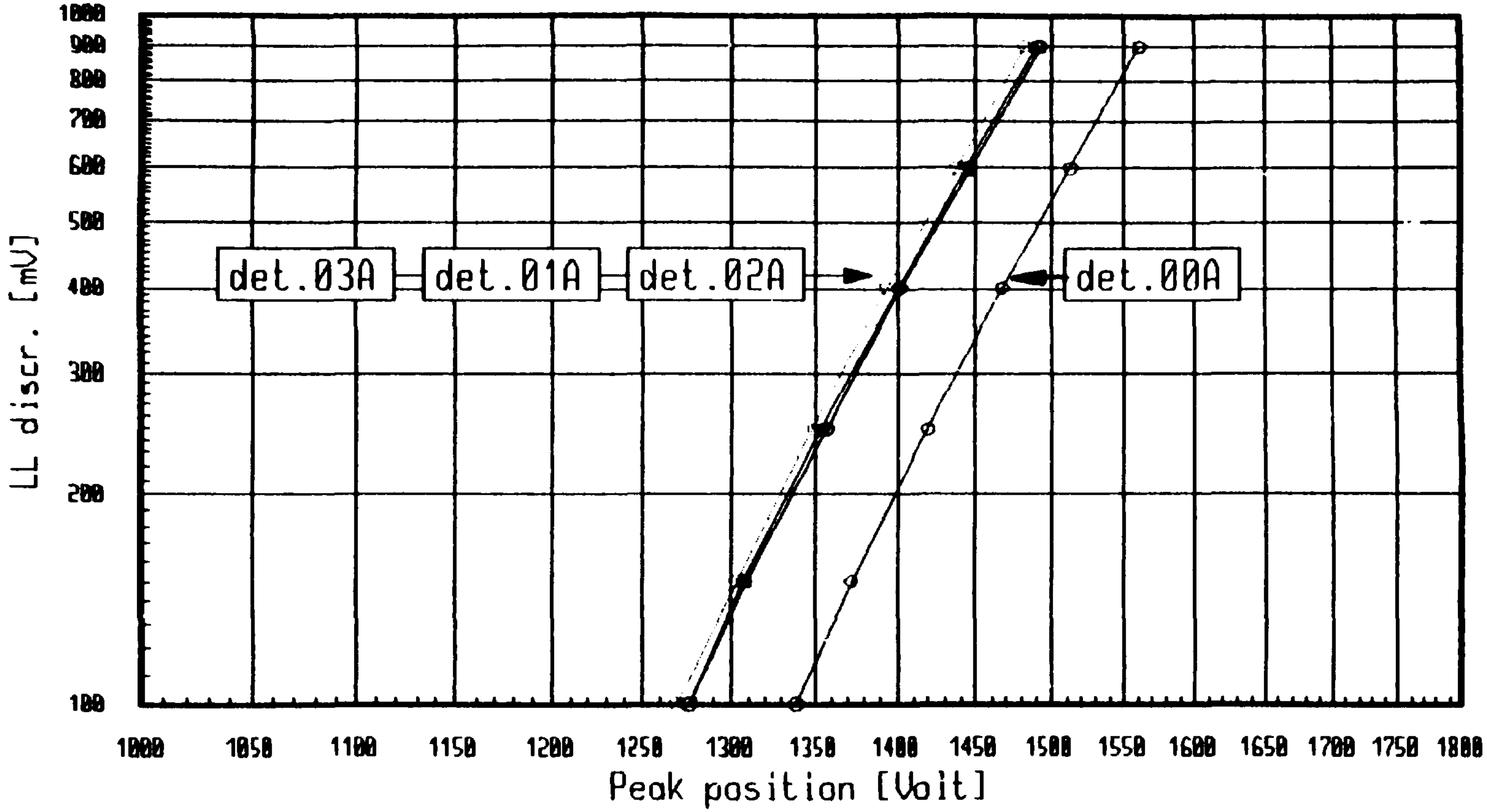

Fig.4a. Calibration lines (LL discriminators) of detectors 00A – 03A.

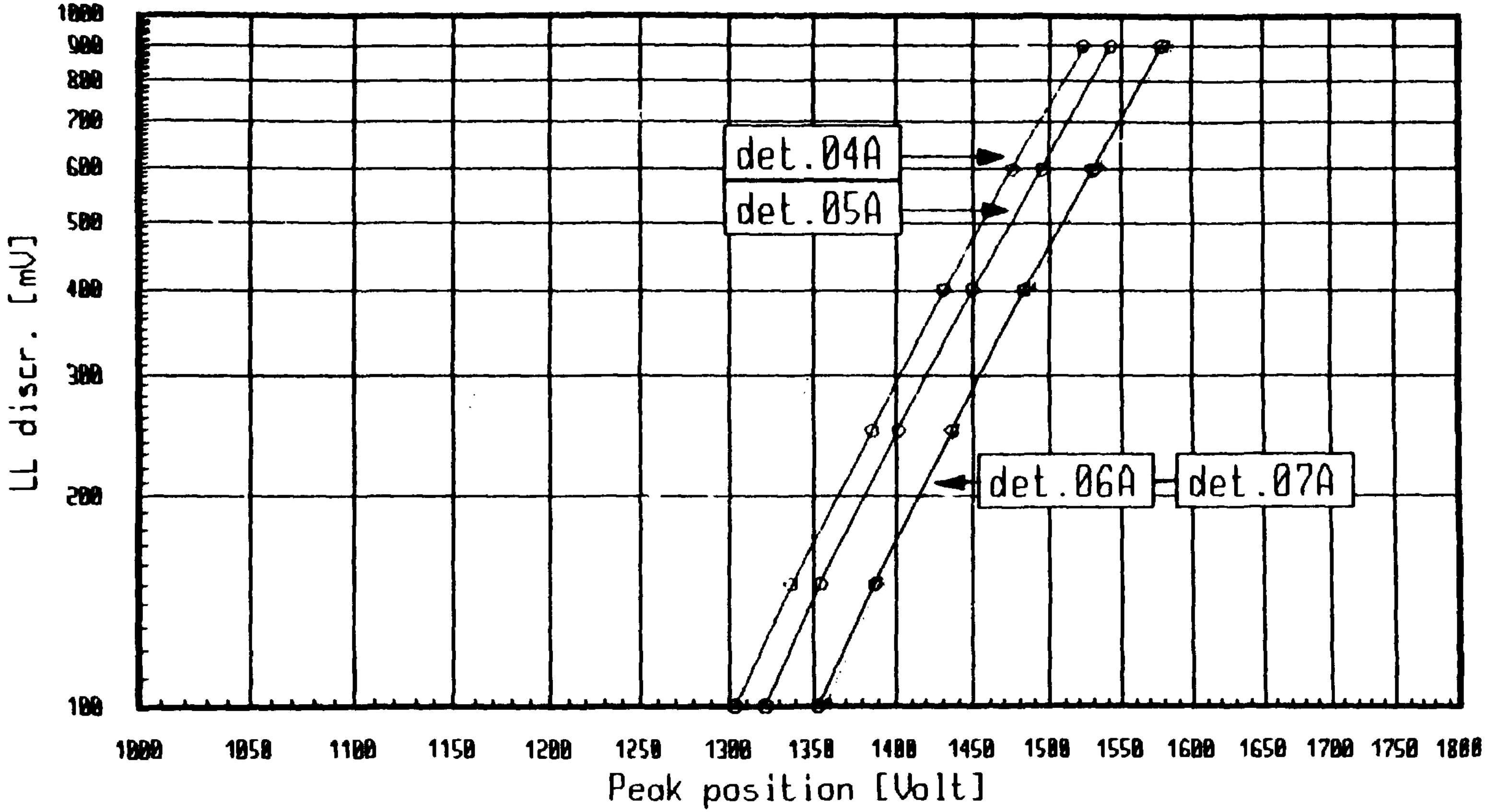

Fig.4b. Calibration lines (LL discriminators) of detectors 04A – 07A.

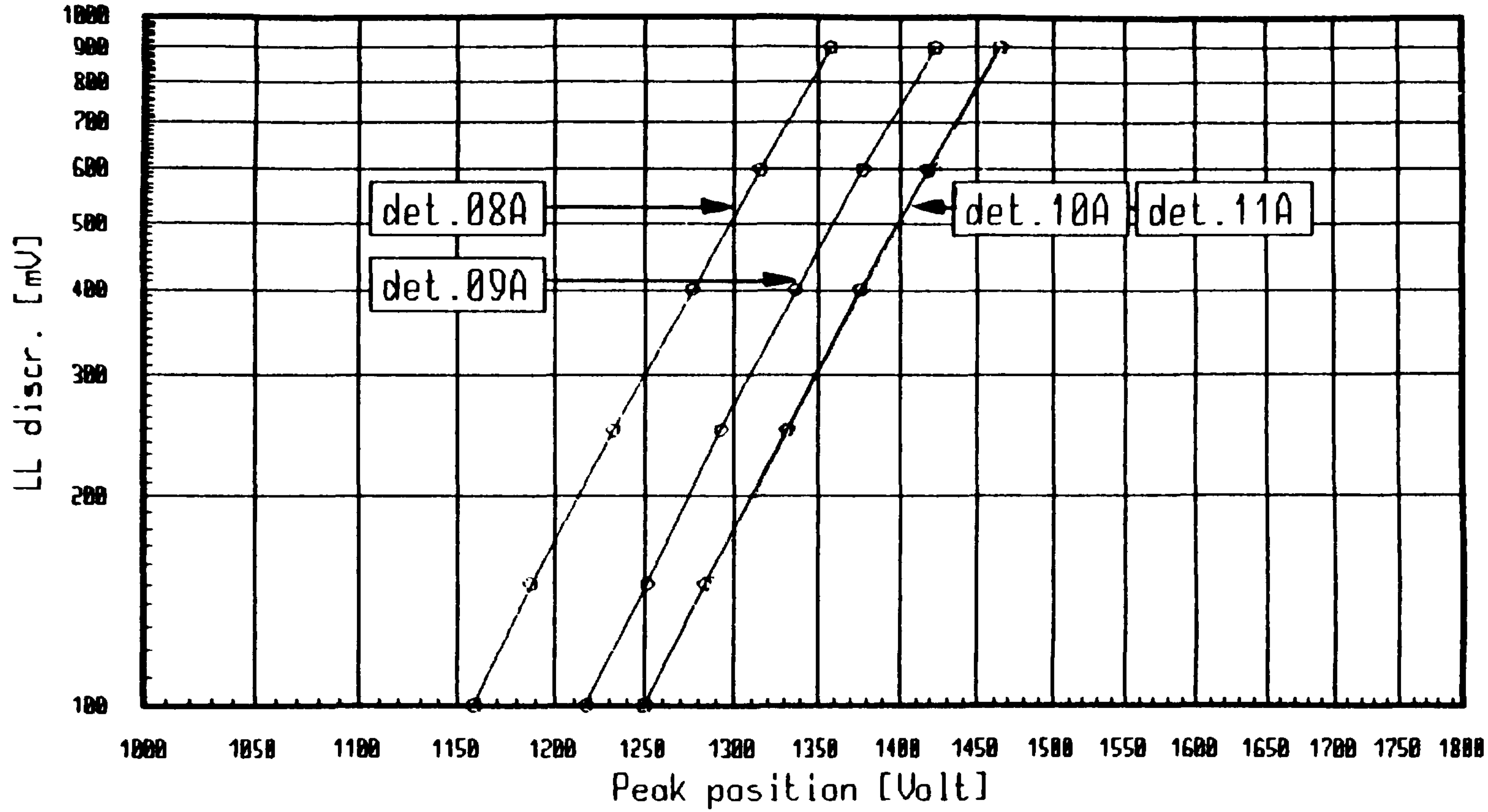

Fig.4c. Calibration lines (LL discriminators) of detectors 08A – 11A.

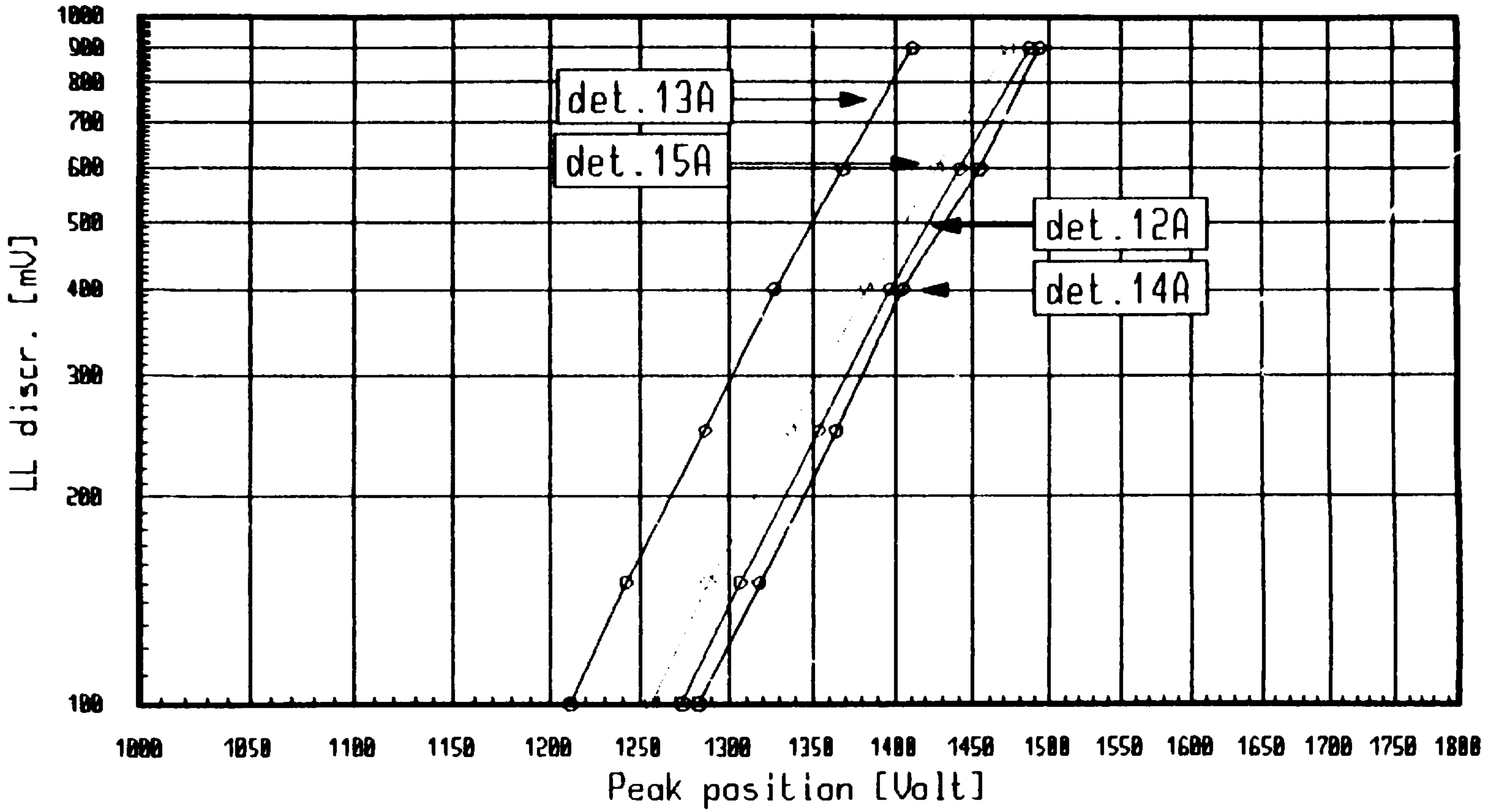

Fig.4d. Calibration lines (LL discriminators) of detectors 12A – 15A.

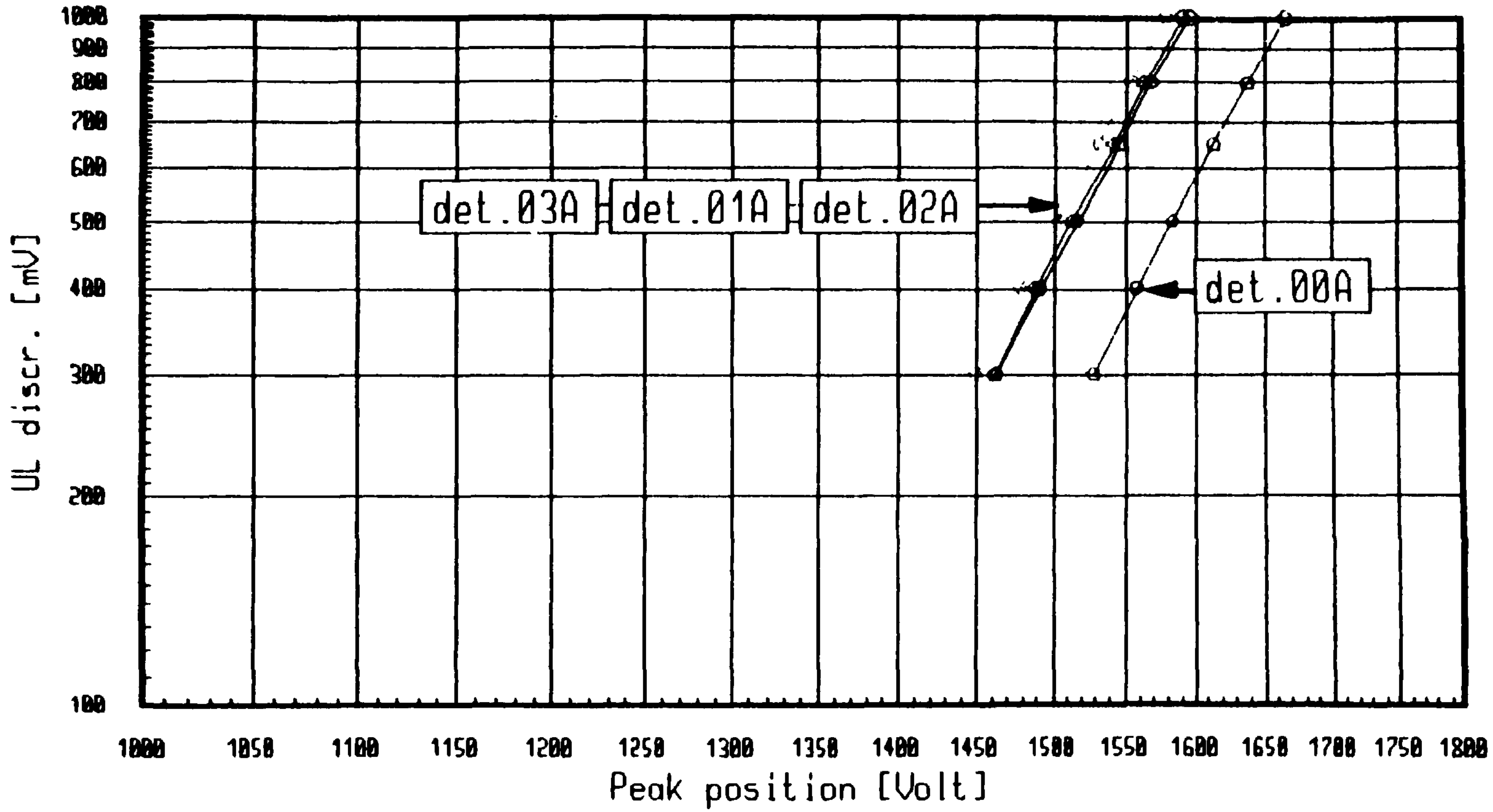

Fig.5a. Calibration lines (UL discriminators) of detectors 00A – 03A.

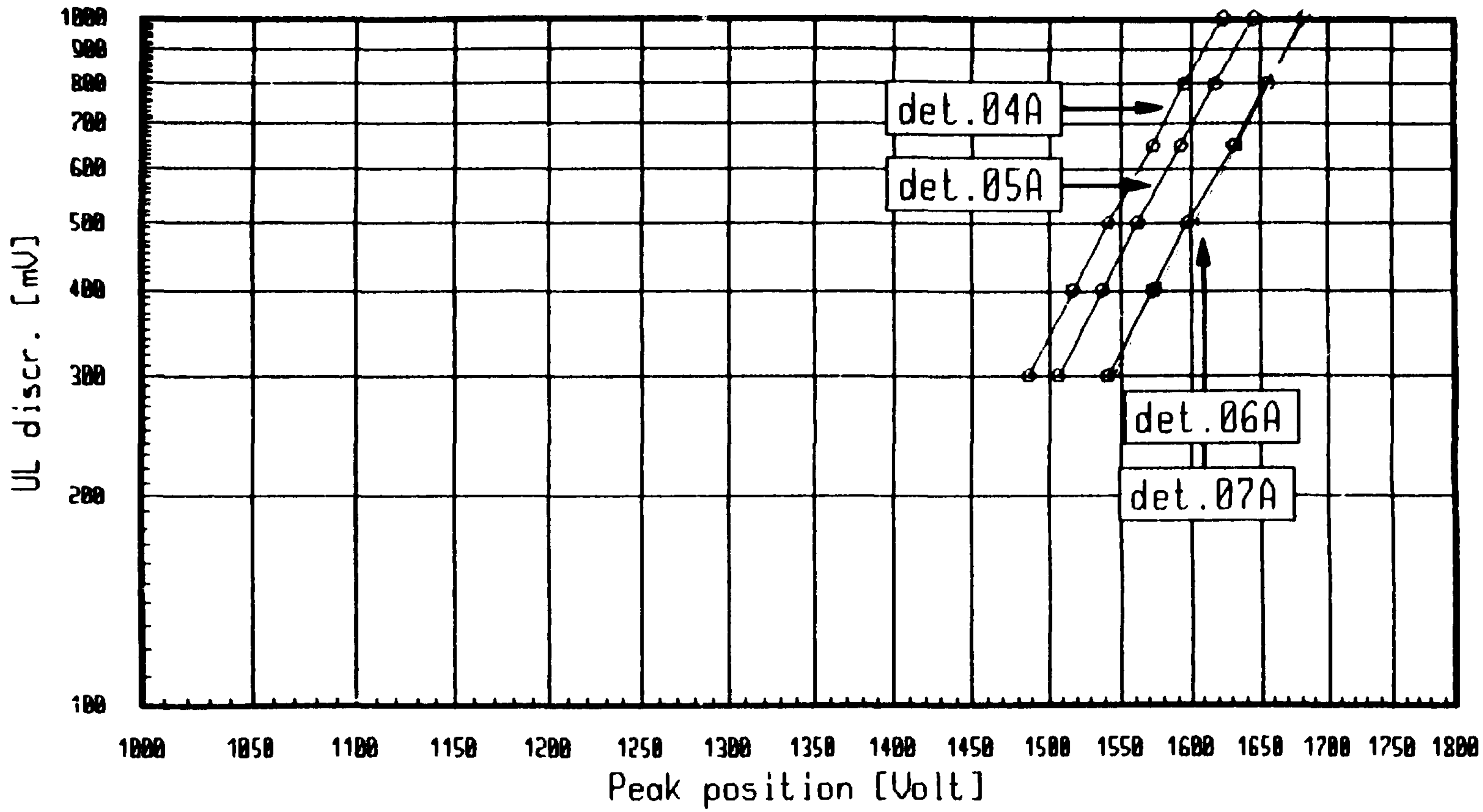

Fig.5b. Calibration lines (UL discriminators) of detectors 04A – 07A.

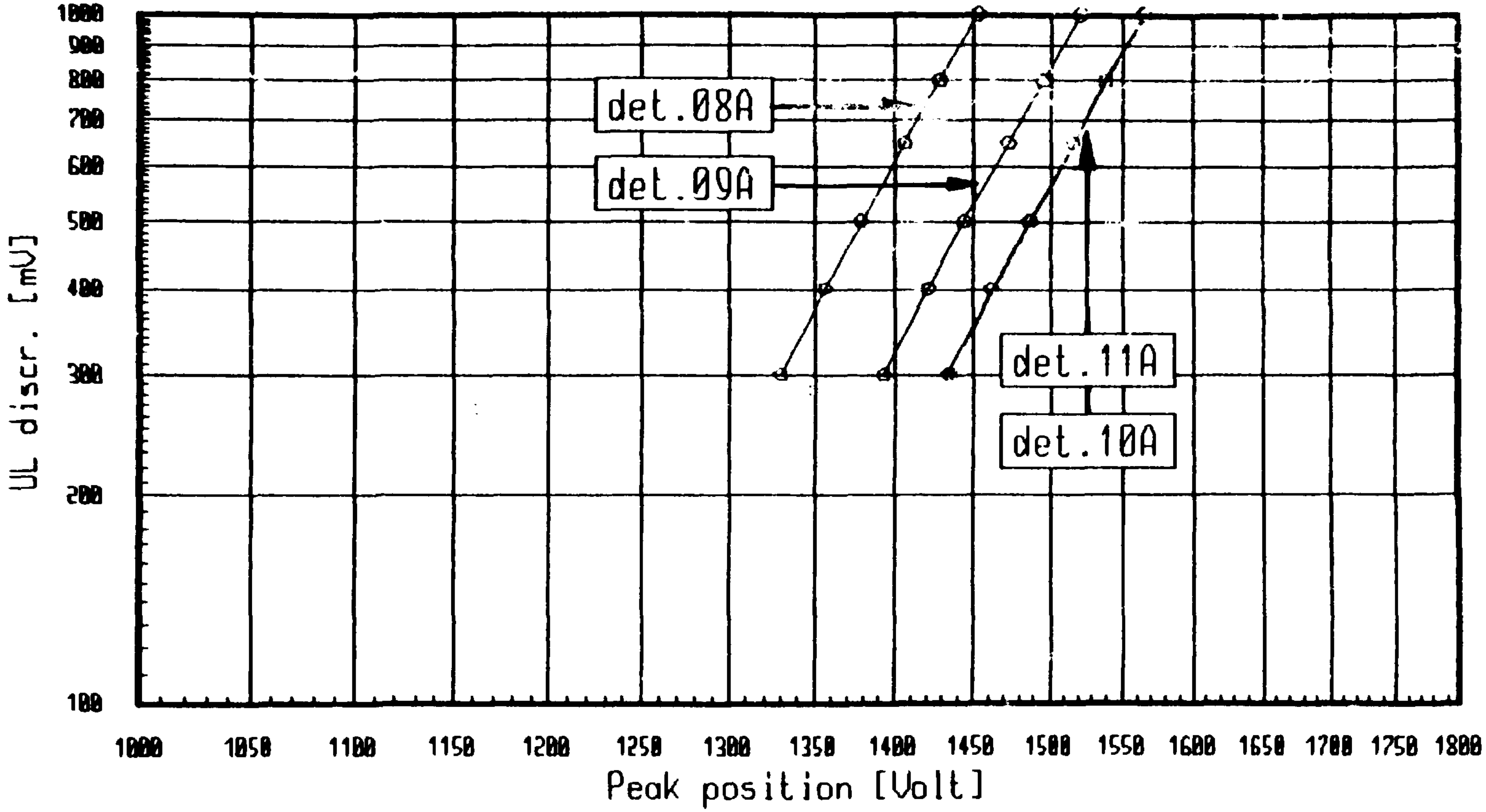

Fig.5c. Calibration lines (UL discriminators) of detectors 08A – 11A.

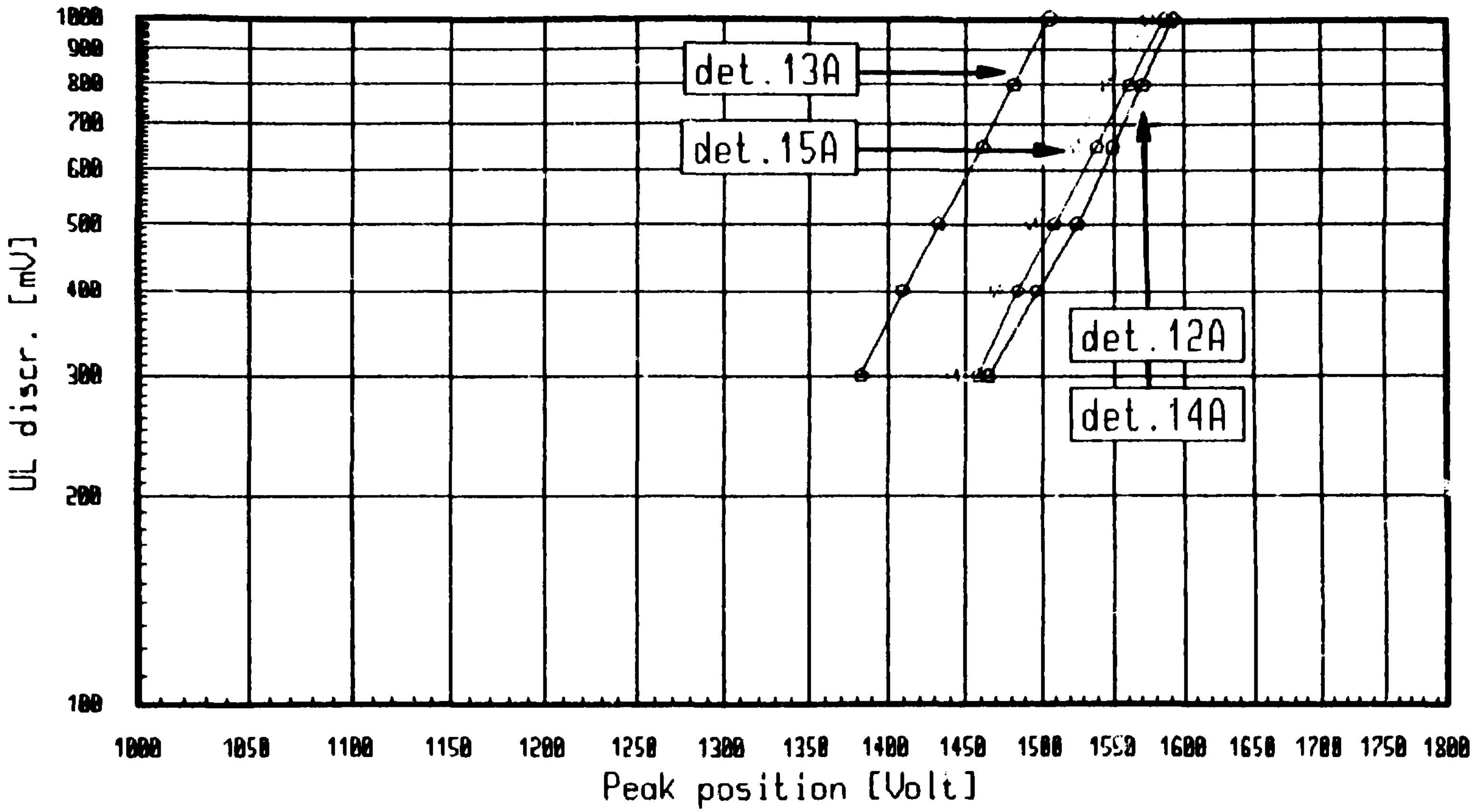

Fig.5d. Calibration lines (UL discriminators) of detectors 12A – 15A.

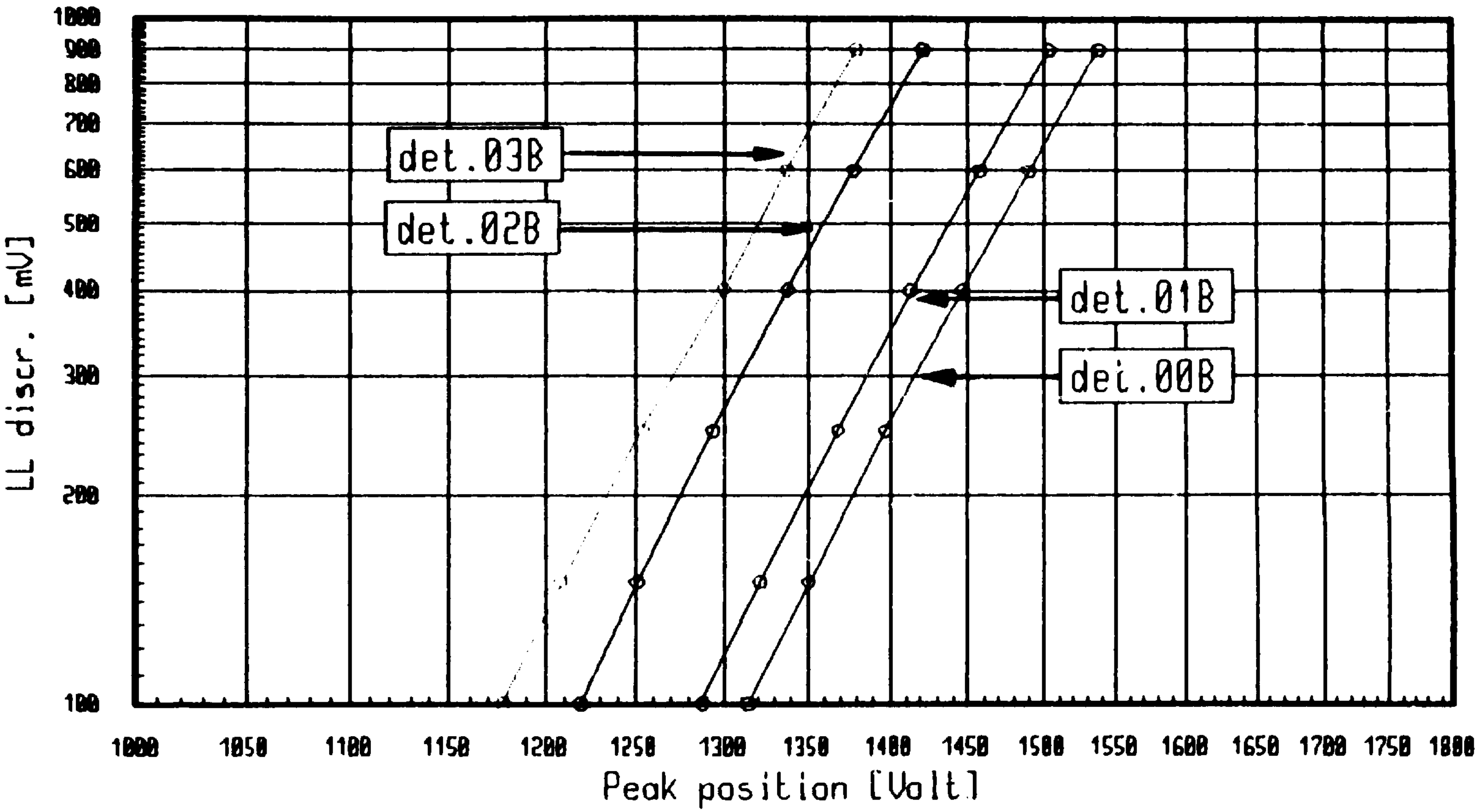

Fig.6a. Calibration lines (LL discriminators) of detectors 00B – 03B.

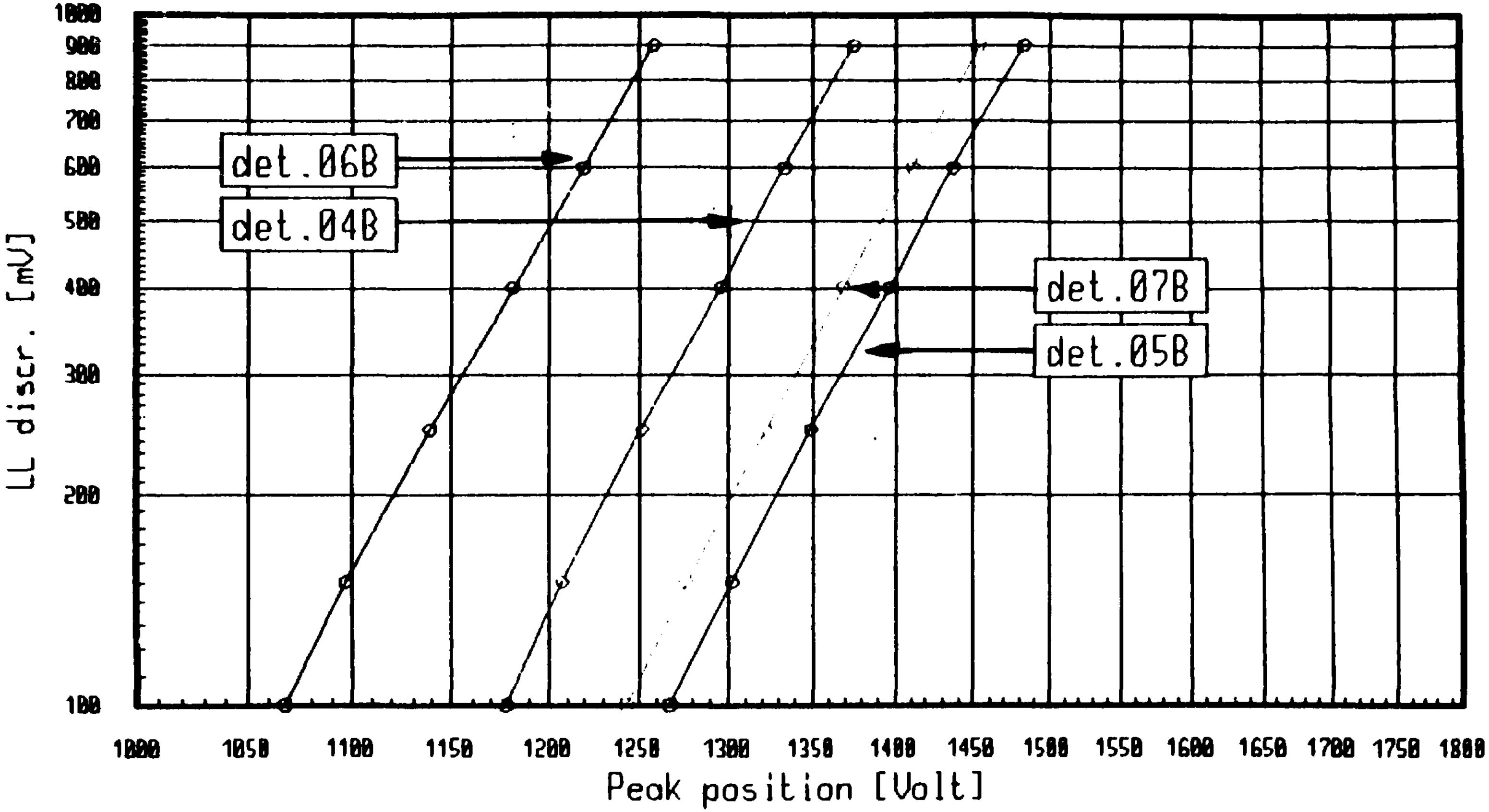

Fig.6b. Calibration lines (LL discriminators) of detectors 04B – 07B.

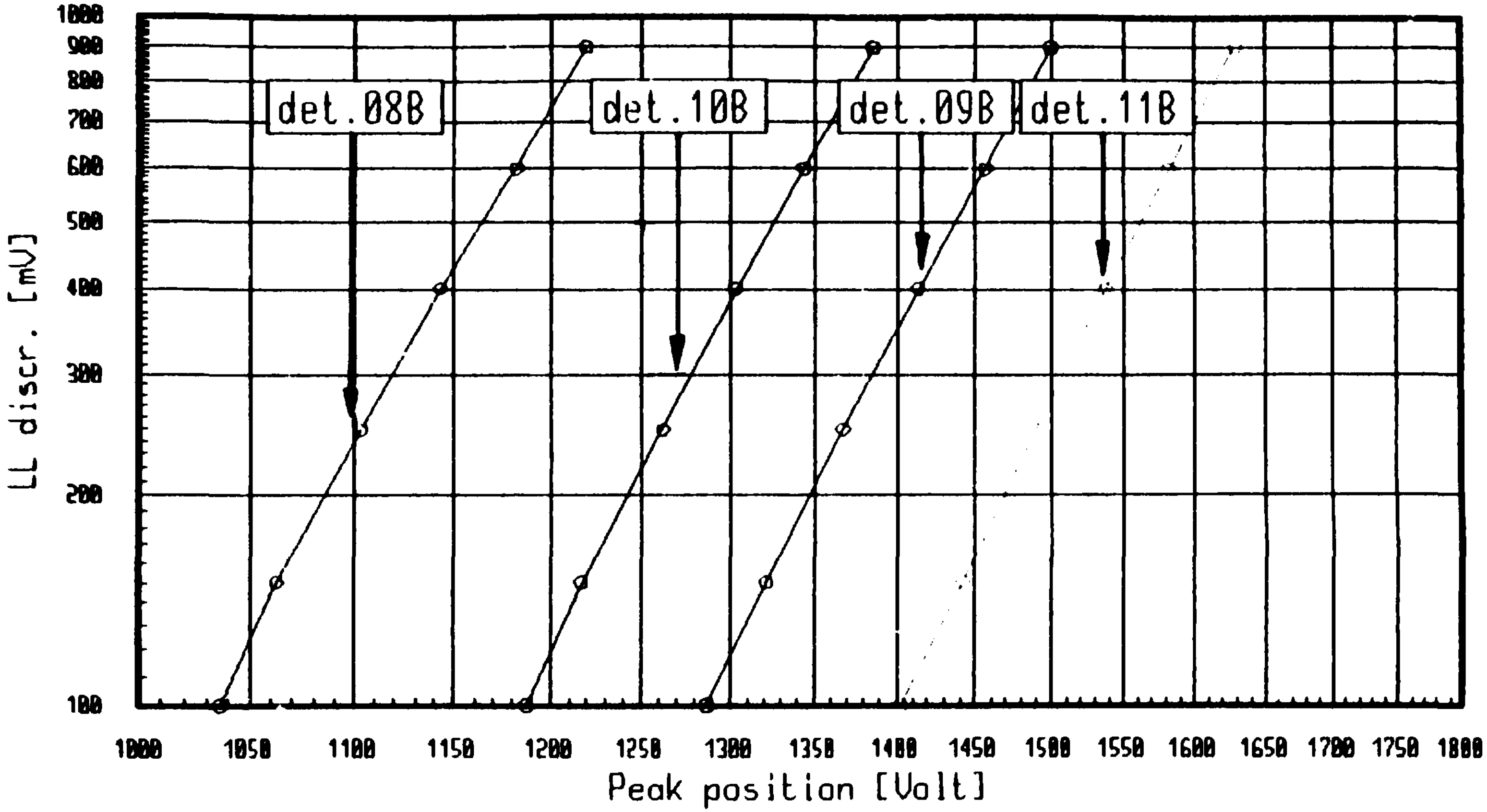

Fig.6c. Calibration lines (LL discriminators) of detectors 08B – 11B.

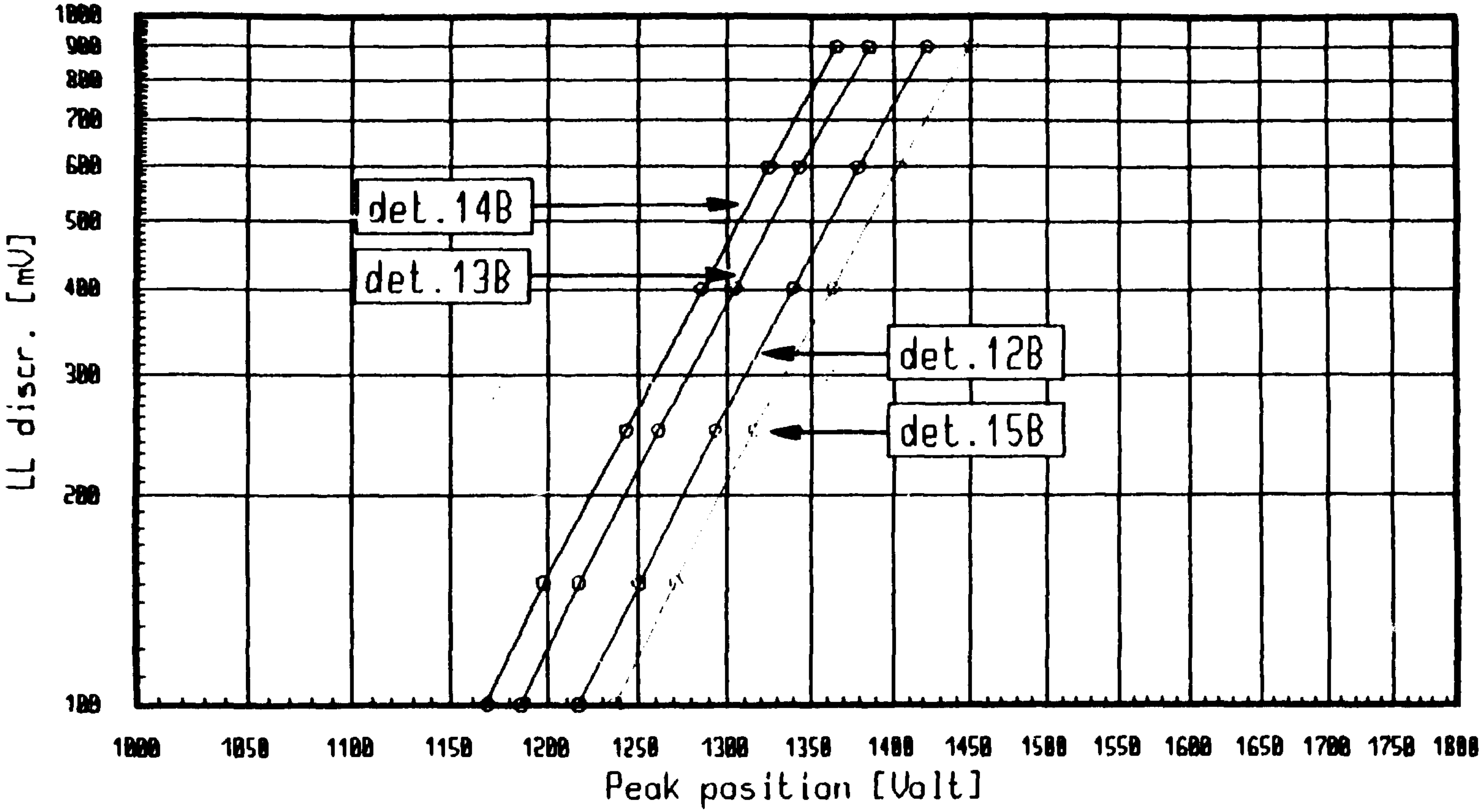

Fig.6d. Calibration lines (LL discriminators) of detectors 12B – 15B.

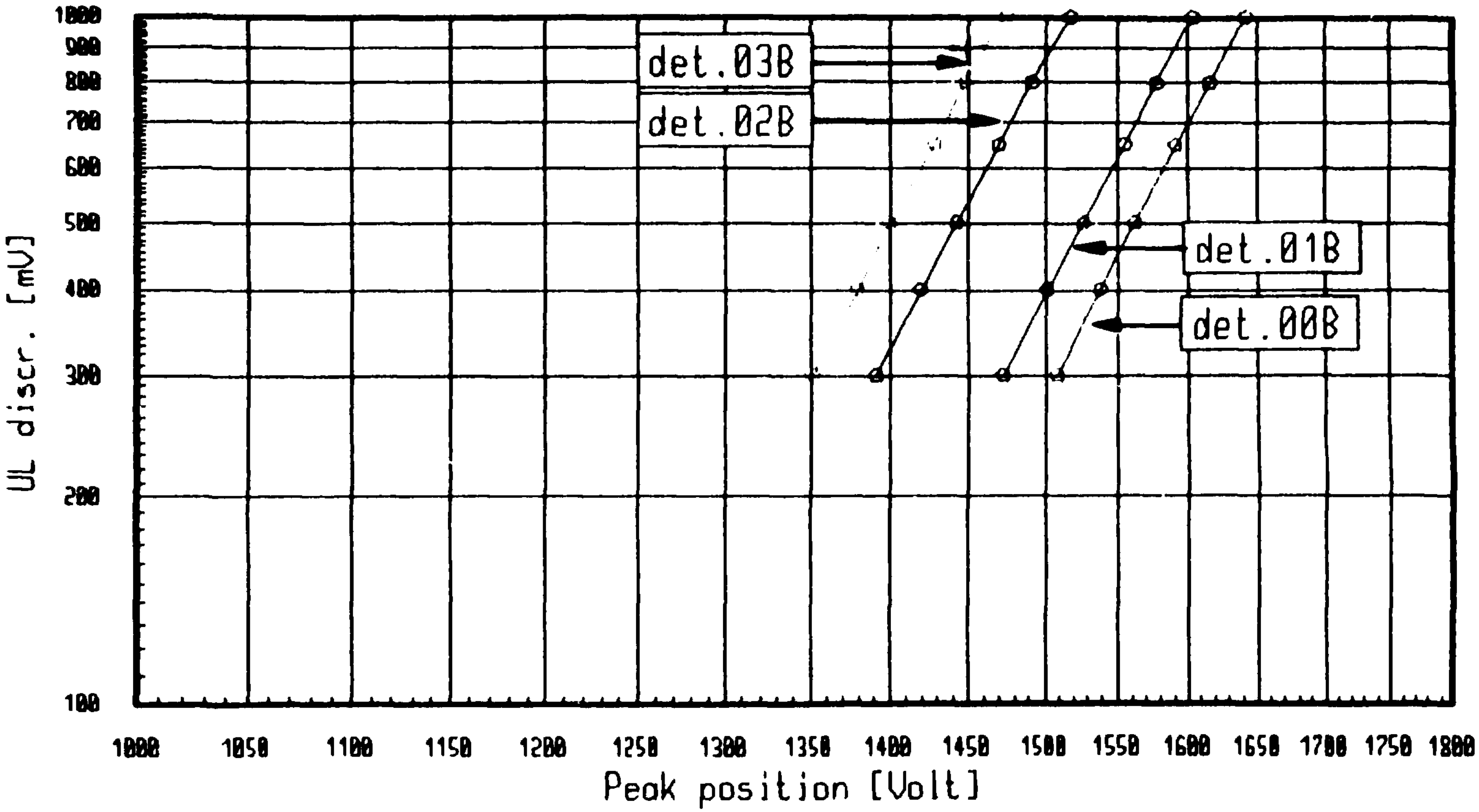

Fig.7a. Calibration lines (UL discriminators) of detectors 00B – 03B.

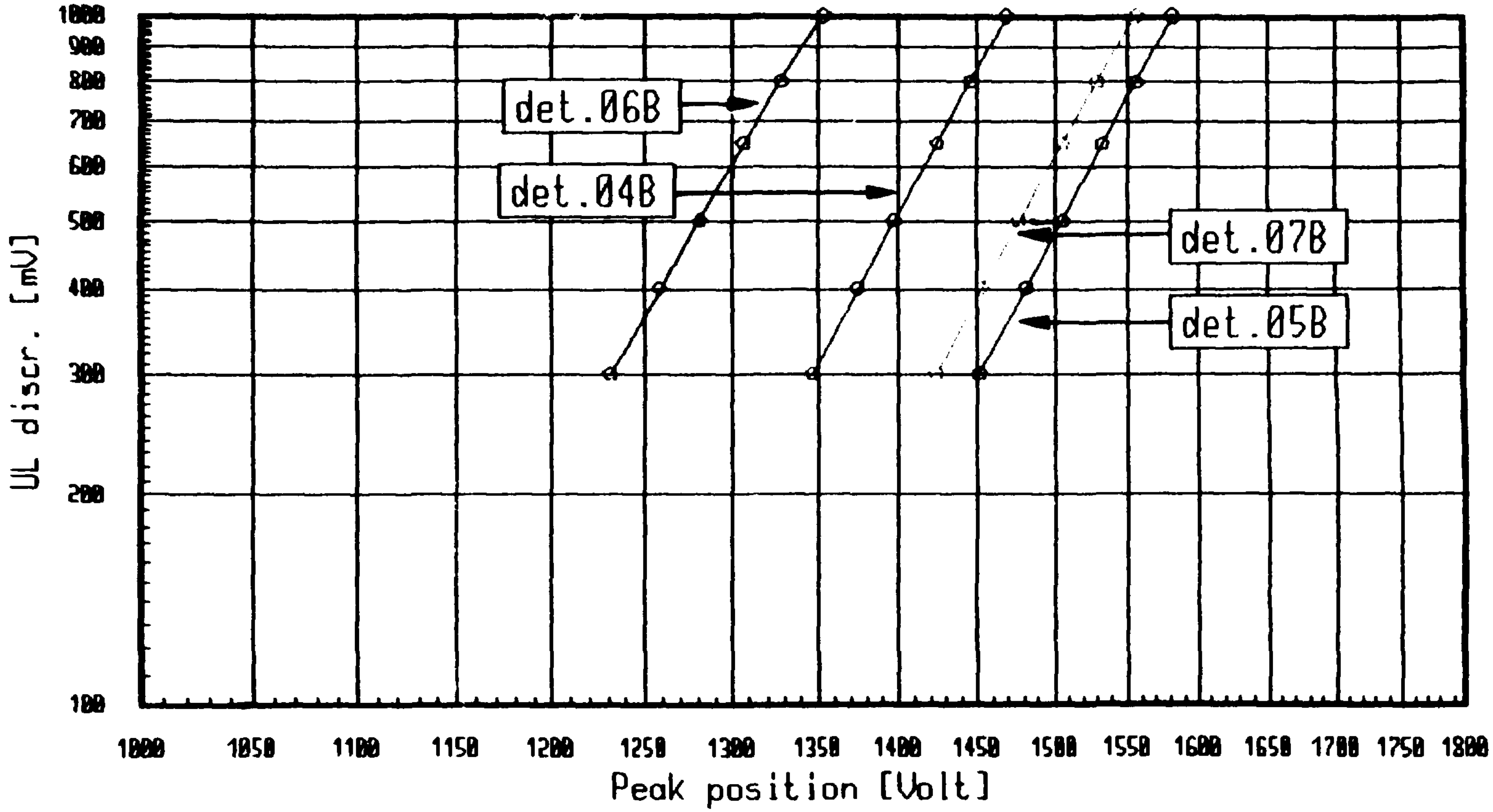

Fig.7b. Calibration lines (UL discriminators) of detectors 04B – 07B.

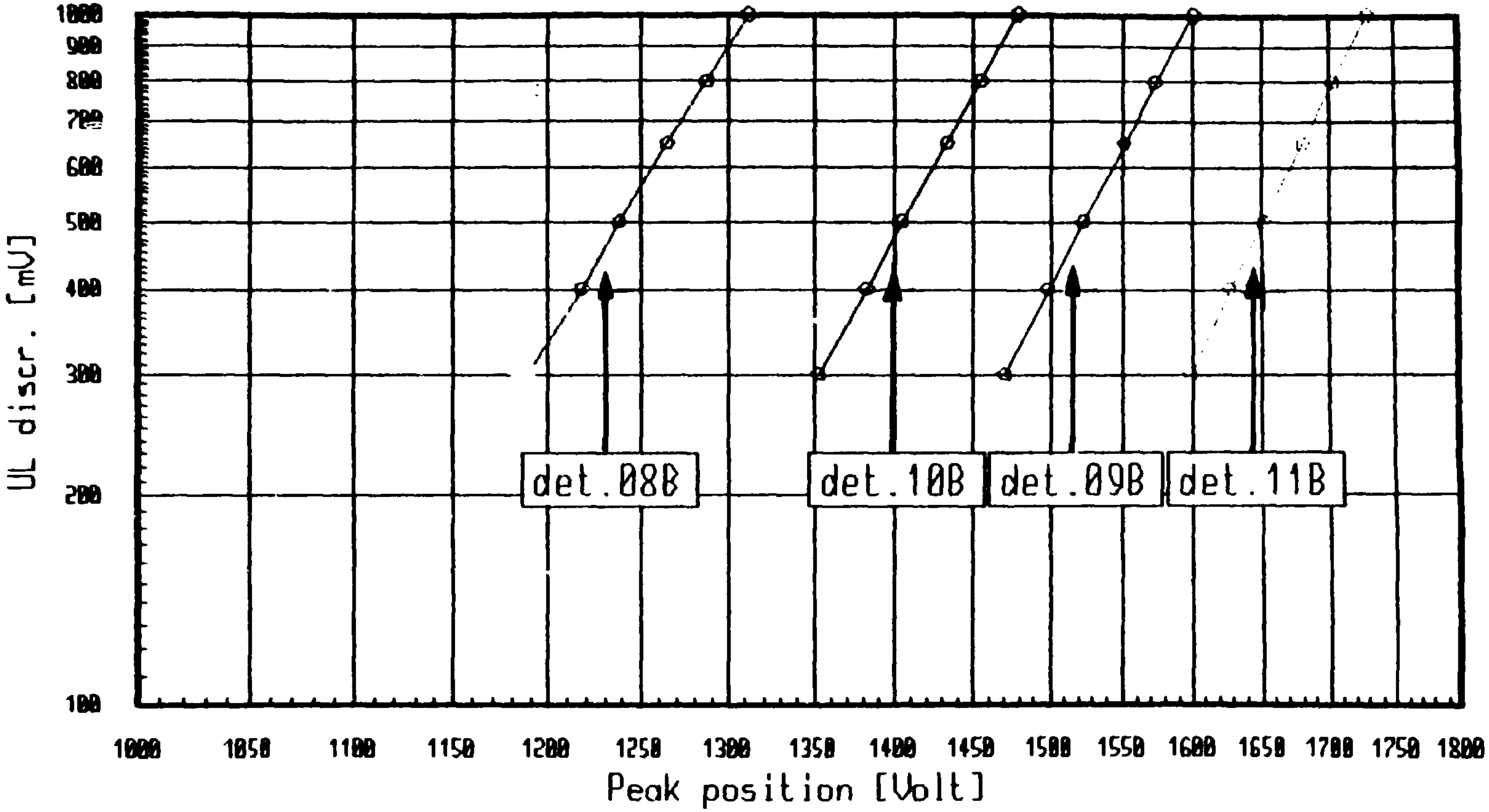

Fig.7c. Calibration lines (UL discriminators) of detectors 08B – 11B.

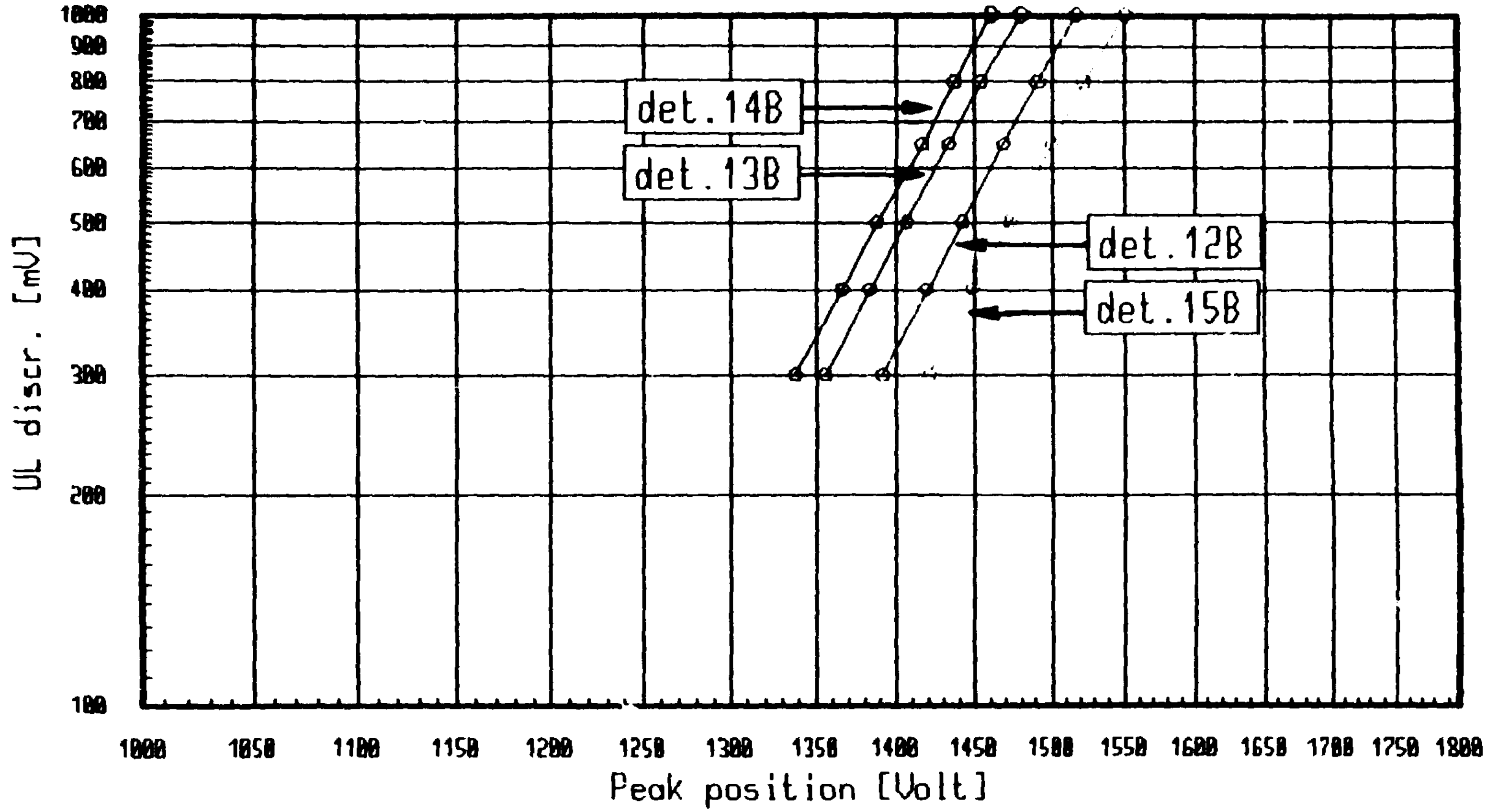

Fig.7d. Calibration lines (UL discriminators) of detectors 12B – 15B.

The calibration parameters K_{0Li}, n_{Li} and K_{0Ui}, n_{Ui} were found for each detector from the linear fit, Eq.(2). The K_{0i} values are different, as expected, and n_i are close to each other. Average values, $\bar{n}_L$ and $\bar{n}_U$, of the LL and UL slopes were calculated and compared. A small difference was found. The experimental points obtained for the LL discrimination D_L = 100 mV for most detectors seem to deviate slightly from a straight line. Fits without these point were also done and then the values $\bar{n}_L$ and $\bar{n}_U$ gave an excellent agreement. Such a behaviour was observed for the detector arrays in both the branches A and B. The comparison is presented in Table 1.

Table 1. Average values of the calibration parameter n for the TANSY neutron detectors

Branch A			Branch B		
$\bar{n}_L$		$\bar{n}_U$	$\bar{n}_L$		$\bar{n}_U$
$\sigma(\bar{n}_L)$		$\sigma(\bar{n}_U)$	$\sigma(\bar{n}_L)$		$\sigma(\bar{n}_U)$
$\bar{\sigma}(n_{Li})$		$\bar{\sigma}(n_{Ui})$	$\bar{\sigma}(n_{Li})$		$\bar{\sigma}(n_{Ui})$
(1)	(2)		(1)	(2)	
14.10	13.78	13.83	14.03	13.77	13.76
0.05	0.05	0.06	0.09	0.10	0.16
0.21	0.21	0.24	0.36	0.41	0.65

(1) when all points are used for the fit

(2) when the points for D_L = 100 mV are rejected

Finally, that variant of the fit when $\bar{n}_L = \bar{n}_U$ (*ie* without the data from D_L = 100 mV) has been chosen and the TANSY neutron detector calibration parameters obtained in that case are listed in Tables 2 and 3. The inidividual values n_{Li} and n_{Ui} are always used in any calculation for the detector settings because they give a much better accuracy than using the mean value (the high voltage $V_i \approx 1400$ is raised to the power $n_i \approx 14$).

The selection of the the data means that the obtained parameters describe well the behaviour of the TANSY neutron detectors for the lower discrimination level not less than 150 mV, and lower settings should not be used. One can expect non–linear effects at lower discrimination.

Table 2. The TANSY neutron detector calibration parameters.

Branch A, Version 0 (06–FEB–90).

Neutron detector parameters: VERSION 0 of 06-FEB-90

det#A	LL K0	LL n	UL K0	UL n
00	(*)-95.52179	13.9199	(*)-95.86216	13.8552
01	-92.98448	13.6593	-97.03045	14.1008
02	-92.67700	13.6140	-94.83014	13.7963
03	-94.71216	13.9067	-96.51661	14.0441
04	-94.02595	13.7617	-94.33855	13.6972
05	-94.15124	13.7548	-93.86630	13.6082
06	-95.71883	13.9254	-93.99732	13.5837
07	-95.37336	13.8737	-97.10278	14.0017
08	-89.64796	13.3720	-92.16994	13.6088
09	-94.05767	13.8962	-92.76257	13.6038
10	-92.60953	13.6415	-92.78299	13.5531
11	-93.63454	13.7802	-94.57716	13.7974
12	-94.35622	13.8519	-97.09632	14.1143
13	-95.02723	14.0444	-95.59081	14.0087
14	(*)-96.57235	14.1437	(*)-98.66975	14.3156
15	-90.92054	13.3984	-92.85490	13.5530

Source: ^{60}Co (E_0 = 781 keV), placed in the geometrical centre of the spectrometer at 1 m distance to each neutron detector.

Units: the parameters correspond to using millivolts for the discrimination levels and volts for the high voltages in Eq.(2).

*) values which are changed later. See paragraph 5 and tables 13 and 14.

Table 3. The TANSY neutron detector calibration parameters.

Branch B, Version 0 (16–MAR–90).

Neutron detector parameters: VERSION 0 of 16-MAR-90

det#B	LL K0	LL n	UL K0	UL n
00	-94.32612	13.7845	-97.53858	14.1077
01	-94.69771	13.8778	-96.95764	14.0739
02	-95.20302	14.0554	-93.84972	13.7565
03	-91.35313	13.5781	-94.32944	13.8779
04	-93.16808	13.8366	-94.18201	13.8629
05	-93.91614	13.7961	-96.26985	14.0069
06	-85.90939	12.9904	-85.23893	12.7811
07	-92.92239	13.6960	-92.48105	13.5235
08	-85.10455	12.9348	-80.74310	12.2098
09	-96.38091	14.1114	-97.91914	14.2092
10	-93.43744	13.8595	-91.37764	13.4656
11	(*)-101.83293	14.6917	(*)-106.93212	15.2696
12	-94.26544	13.9245	-94.83786	13.8927
13	-93.53030	13.8722	-93.36443	13.7377
14	-92.13696	13.7060	-93.20802	13.7402
15	-92.13000	13.5939	-94.02959	13.7413

Source: ^{60}Co (E_0 = 781 keV), placed in the geometrical centre of the spectrometer at 1 m distance to each neutron detector.

Units: the parameters correspond to using millivolts for the discrimination levels and volts for the high voltages in Eq.(2).

*) values which are changed later. See paragraph 5 and tables 13 and 14.

3. Determination of E_0 for ^{60}Co.

The ^{60}Co energy E_0 has been defined as the peak position of the amplitude distribution when the Compton edge energy E_C has been chosen to the half–peak position (*cf* Fig.11 in [1] and see for related problems in [5]). ^{60}Co emits γ quanta of two energies, $E_{\gamma1}$ = 1173 keV and $E_{\gamma2}$ = 1332 keV, which give the corresponding Compton energies E_{C1} = 963 keV and E_{C2} = 1118 keV. These energies are not resolved due to limited resolution of the scintillator and appear in a measurement as if there was only one energy. One can use a weighted value E_γ = 1253 keV (*cf* [5]) which gives the Compton edge energy E_C = 1041 keV. But the peak position of the amplitude distribution in such a situation depends on the type of the scintillator used and on the source to detector distance. The relation between peak E_0 and half–peak E_C positions is not given directly. Therefore we measured experimentally E_0 for the ^{60}Co source.

We used a common energy calibration procedure . The ^{22}Na, ^{207}Bi, and ^{137}Cs sources were used. The Compton edge energies E_C were assumed to be at the half–peak positions to get the energy scale. Then the ^{60}Co energies E_0 and E_C were determined from the amplitude distribution measurement. The energies E_0 of other sources were also obtained for comparison.

While repeating such a measurement for another detector we found the determined energy E_0 for ^{60}Co to be significantly different in spite of a very good linearity of the energy scaling and reproducibility of other results in both the cases. Therefore the amplitude distribution measurements were done for several detectors at different high voltages to determine the energy E_0 with high accuracy. The choice of the neutron detectors was as follows: one of an average sensitivity (12B), one of a high sensitivity (08B) and one of a low sensitivity (00B). The choice gave one detector in the middle of the array and two detectors to the left side, *cf* Fig.8. Then a fourth detector on the right side (07B) was included in the measurements.

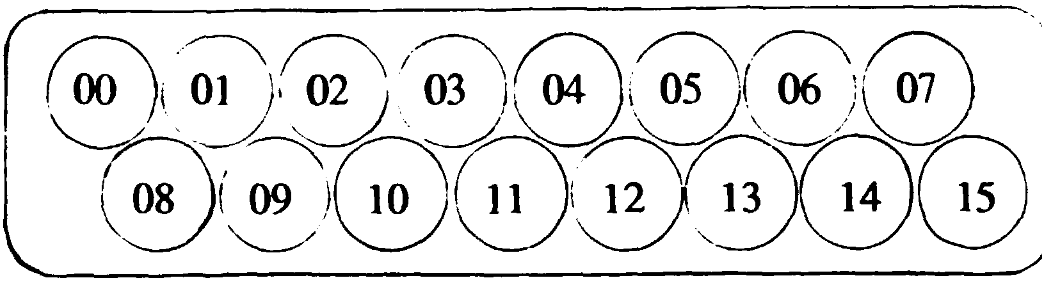

Fig.8. Scheme of the positions of the TANSY neutron detectors as seen from the centre of the spectrometer (for both branches A and B).

Each detector was used with two different high voltages (one corresponding to an approximated value of the operation voltage and the second one with voltage decreased to give an amplification of 0.8). The energies E_0 and E_C were found in each case and mean values were calculated. The results of individual measurements for the ^{60}Co source are given in Table 4.

Table 4. Individual results of the measurement of ^{60}Co energies E_0 and E_C.

Measurement	Detector	Experim. code	E_C (keV)	E_0 (keV)
1	12B	H318	1029	776
2		H321	1011	780
3	00B	H319	1040	752
4		H322	1037	732
5	08B	H320	1045	793
6		H323	1057	805
7	07B	H325	1055	803
8		H326	1060	807

Examples of the positions of the two energies against channels are shown in Figs 9 and 10 for the two cases of being the closest and the most distant from the means. The obtained mean energies for all sources used are listed in Table 5.

Table 5. Results of the measurements of the energies E_0.

Source	Calculated E_γ (keV)	E_C (keV)	Measured $\bar{E}_{Cm}$ $\sigma(E_{Cm})$ (keV)	$\bar{E}_0$ $\sigma(E_0)$ (keV)	Δ_C (%)
^{22}Na	1274.5	1062	1060 3	814 25	−0.2
	511.0	341	342 2	253 6	0.3
^{137}Cs	661.6	477	477 2	365 11	0.0
^{207}Bi	1063.6	858	862 4	658 16	0.5
	569.7	393	391 1	292 7	−0.5
^{60}Co	1253.0*)	1041	1042 16	781 27	——

*) weighted mean energy [5]

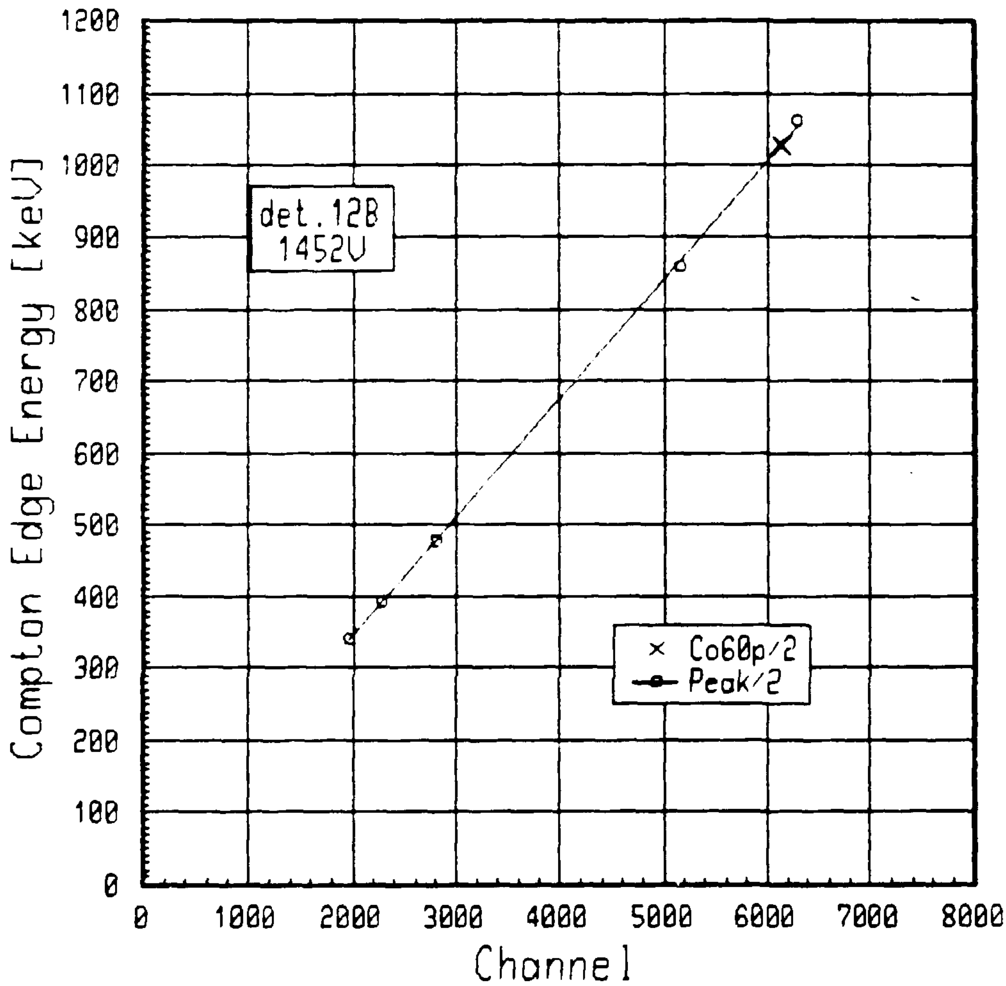

Fig.9. Half–peak positions (E_C) of the amplitude distributions of the used calibration γ sources (o) and of ^{60}Co (x) . A normal position of the ^{60}Co half–peak.

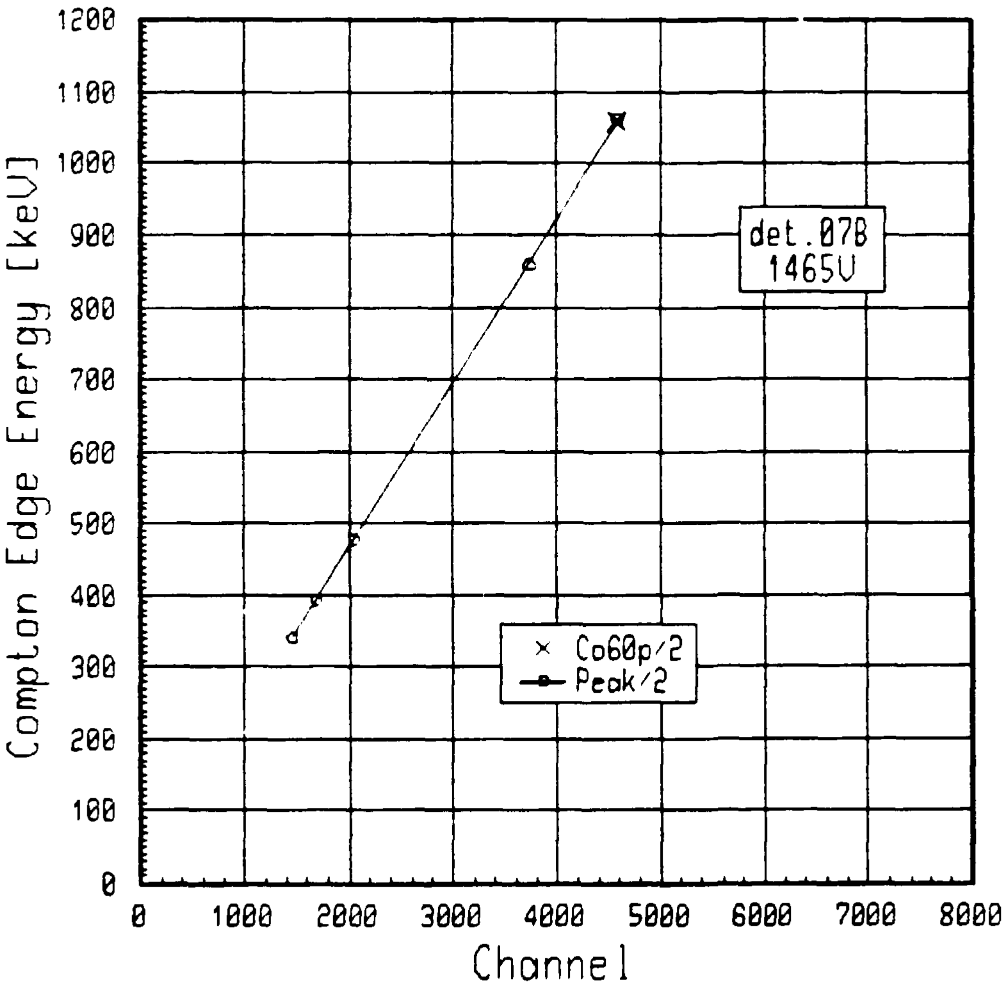

Fig.10. An example of an extremely deviating position (x) of the ^{60}Co half–peak (almost coinciding with the higher half–peak position for ^{22}Na). Note the excellent linearity of the energy scale based on the calibration sources (o).

A relative deviation Δ_C of the "measured" energy $\bar{E}_{Cm}$ (*ie* mean of the individual values obtained from the fits) from the true Compton edge energy, E_C, (calculated from E_γ) for the used reference sources was defined:

$$\Delta_C = \frac{\bar{E}_{Cm} - E_C}{E_C} \quad . \tag{3}$$

Eq.(3) is a measure of the precision of the determination of the ^{60}Co energy E_Q . A very good agreement of the E_C and mean $\bar{E}_{Cm}$ values for all sources was obtained (*cf* Table 5) although divergencies in individual cases could be observed to be greater (the highest one for ^{22}Na 1062 keV was –7 keV). The standard deviations for the obtained mean $\bar{E}_0$ energies are greater, which is partly due to a more inaccurate determination of the amplitude peak position than of its half–height. The measured Compton edge energy for the ^{60}Co source, $\bar{E}_{Cm}$ = 1042 keV is in full agreement with the theoretical value E_C calculated from the weighted energy E_γ (*cf* Table 5). The standard deviation $\sigma(E_C)$, greater than for other sources, reflects greater differences in the individual results E_C for ^{60}Co (*cf* Table 4). The above analysis of the results allows us to accept the measured ^{60}Co energy E_0 = 781 keV (energy distribution peak) as a calibration constant E_0 which is used in calculation of settings for the TANSY neutron detectors. However, because the individual results E_0 differ significantly (*cf* Table 4), one can expect for some detectors small deviations from true (unknown) settings.

4. Test measurements

4.1. Check of the Obtained Calibration Parameters

A check of the neutron detector parameters obtained from the calibration procedure (as shown in paragraph 2) seems to be desirable to detect any mistake in handling numerous data in consecutive steps of the method. Such a check is very easy to perform. One can assume a discrimination level D and run a count rate distribution measurement as for the calibration (the same source, the same geometry). The peak positions in the differentiated distributions, $(V_{Pm})_i$, are found. For the same discrimination level the peak positions can be calculated from Eq.(2):

$$\ln(V_{Pt})_i = \frac{1}{n_i} [\ln(D) - K_{0i}] , \tag{4}$$

where K_{0i} and n_i are the obtained parameters for the i^{th} detector. The calculated and measured values should agree. The parameters are confirmed if the differences fulfil the condition:

$$| (V_{Pm})_i - (V_{Pt})_i | \leq \Delta V_P . \tag{5}$$

The limit value has been fixed to $\Delta V_P = 5V$ from an experience achieved during the elaboration of the method. There are several reasons for this value of ΔV_P. The high voltage step is 5V (the digital control of the high voltage limit allows a precision of 1V and the accuracy of the unit is *ca* 1.5V). Statistical differencies between two measurements immediately following each other give about 2V deviations. Fluctuations of the discrimination and DC levels increase the deviations to 3 or 4 volts. Finally, the peak position is defined within an interval of *ca* 5V.

4.2 Test by Amplitude Distribution Measurements

In our experimental setup it is impossible to get an amplitude distribution of the fast signal (A) used in the system, which could be the best check of the calibration, because the signal is too fast (ns) for an Analog to Digital Converter (ADC). One can use another output signal from the PM–base, a linear signal (B) which should have an amplitude proportional to the signal A. Then it is possible to register by the ADC the amplitude distribution of the signal B while the discriminated signal A triggers a gate for the ADC. The method has been described and illustrated in Figs 13 and 14 in [1]. A typical result of such measurements is shown in Fig.11 where in the distribution of signal B the cut lines coming from several different discrimination levels of signal A are observed. When the amplitude distribution B was earlier scaled to energy (the procedure with ^{22}Na, ^{137}Cs, ^{207}Bi sources) the energy corresponding to the discrimination levels was found. However, there are some problems. The discrimination line is not sharp (not vertical in the plot) but has a slope which gives an interval in channels, *ie* in energy. The intervals in the example in Fig.11 correspond to such large values as 45 keV at lower discrimination level D_L = 150 mV or 91 keV at D_L = 500 mV, and for the upper level they are even larger. We decided to use the half–height position (which is always well defined) as the point corresponding to the discrimination level. The second question is whether the signals A and B are really strictly proportional. Examples of the results of the measurement: discrimination line position in the amplitude distribution B *versus* discrimination level for signal A are given in Fig.12 (LL discriminator) and Fig.13 (UL discriminator). One can notice that the dependence is perfectly linear but the zero discrimination level is observed in non–zero channel. That means that proportionality between the signals A and B is disturbed for some reasons. One reason we know of is the uncertainty of the position of the discrimination cut–line. Also a non–linearity of the amplitude signal at low energies can be observed as offset values which are different for the two signals because they are shaped in different electronic circuits in the PM–base).

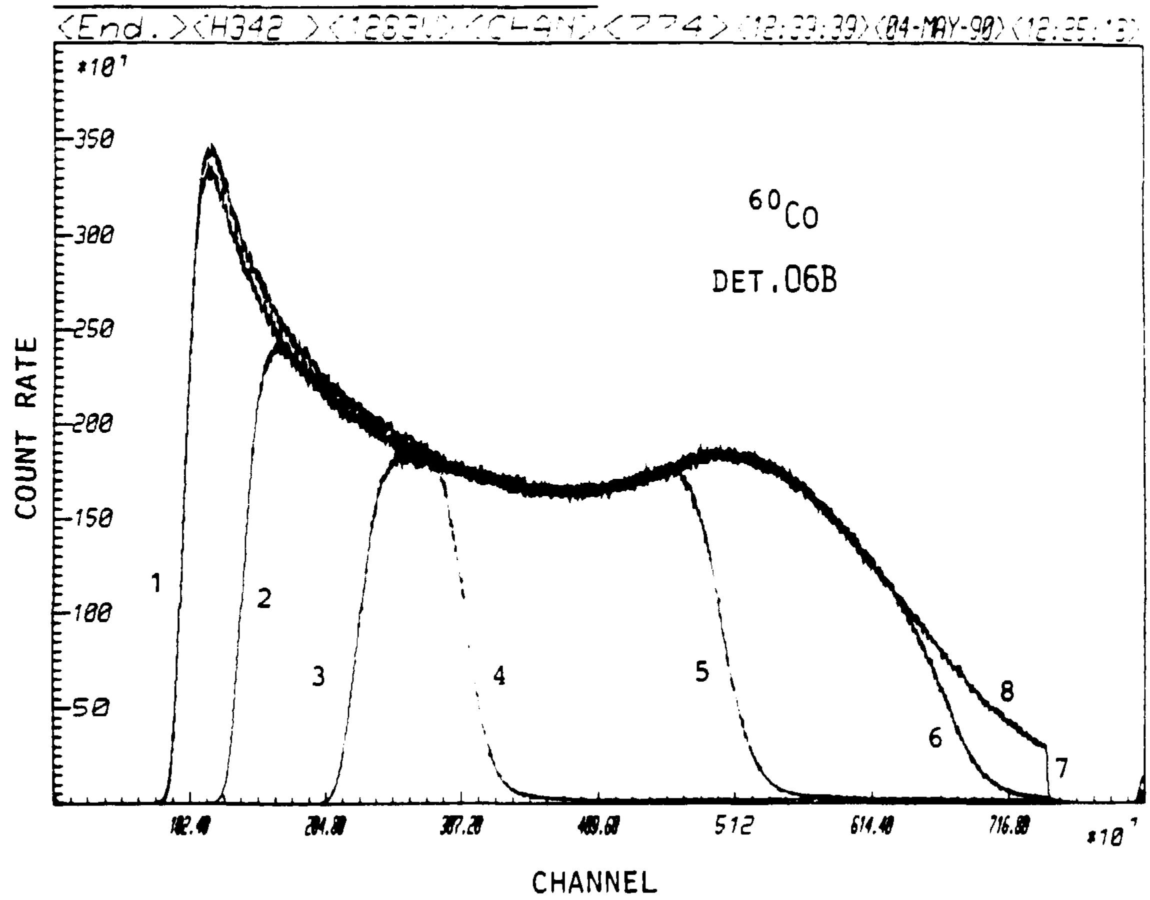

Fig.11. Amplitude distributions of linear signal B controlled by the discriminated fast signal A (see the electronic setup in Fig.13 in [1]). Discrimination levels in mV: 1) $D_L = 200$, 2) $D_L = 300$, 3) $D_L = 500$, 4) $D_U = 300^*$, 5) $D_U = 510^*$, 6) $D_U = 700^*$, 7) internal discrimination by the ADC, 8) distribution without discrimination.

(* - attenuated signal A).

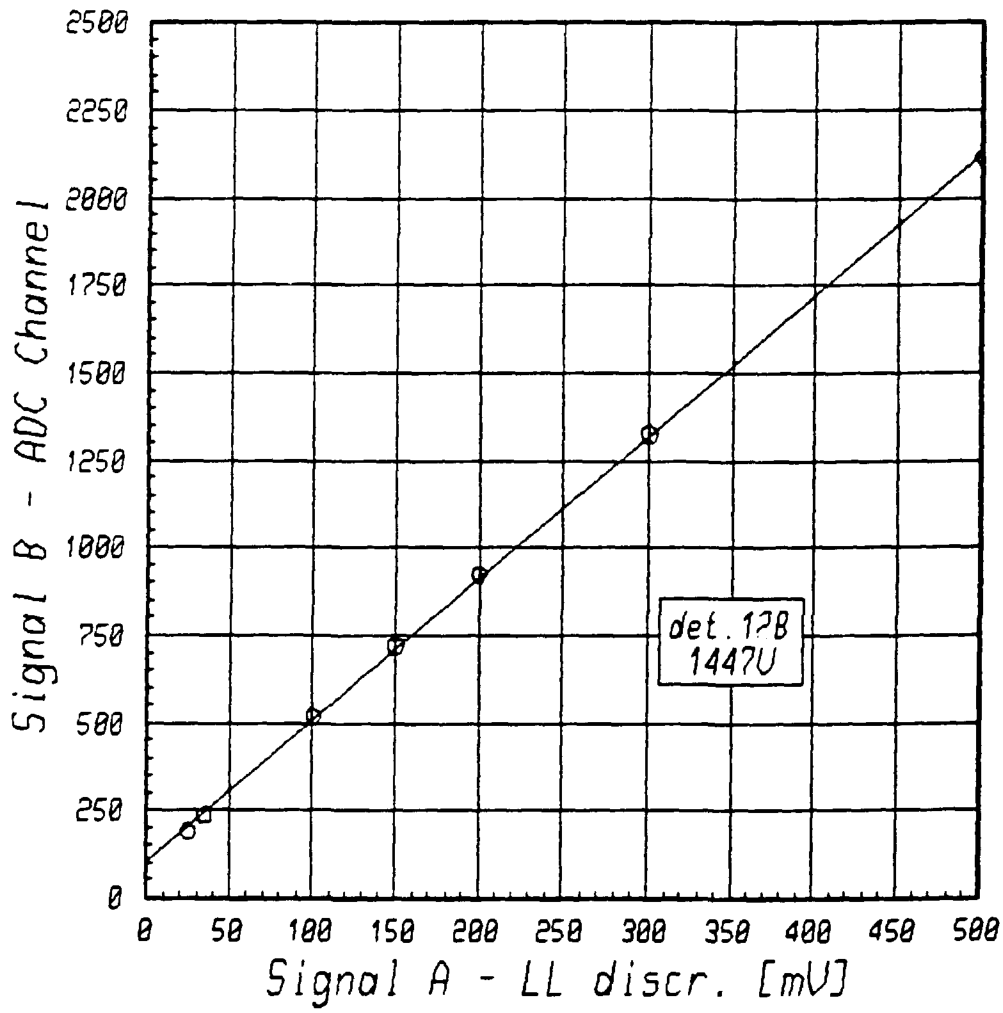

Fig.12 Position (channel) of the discrimination line in the distribution of linear signal B as a function of the discrimination level of fast signal A (Branch B, detector 12B, LL discriminator).

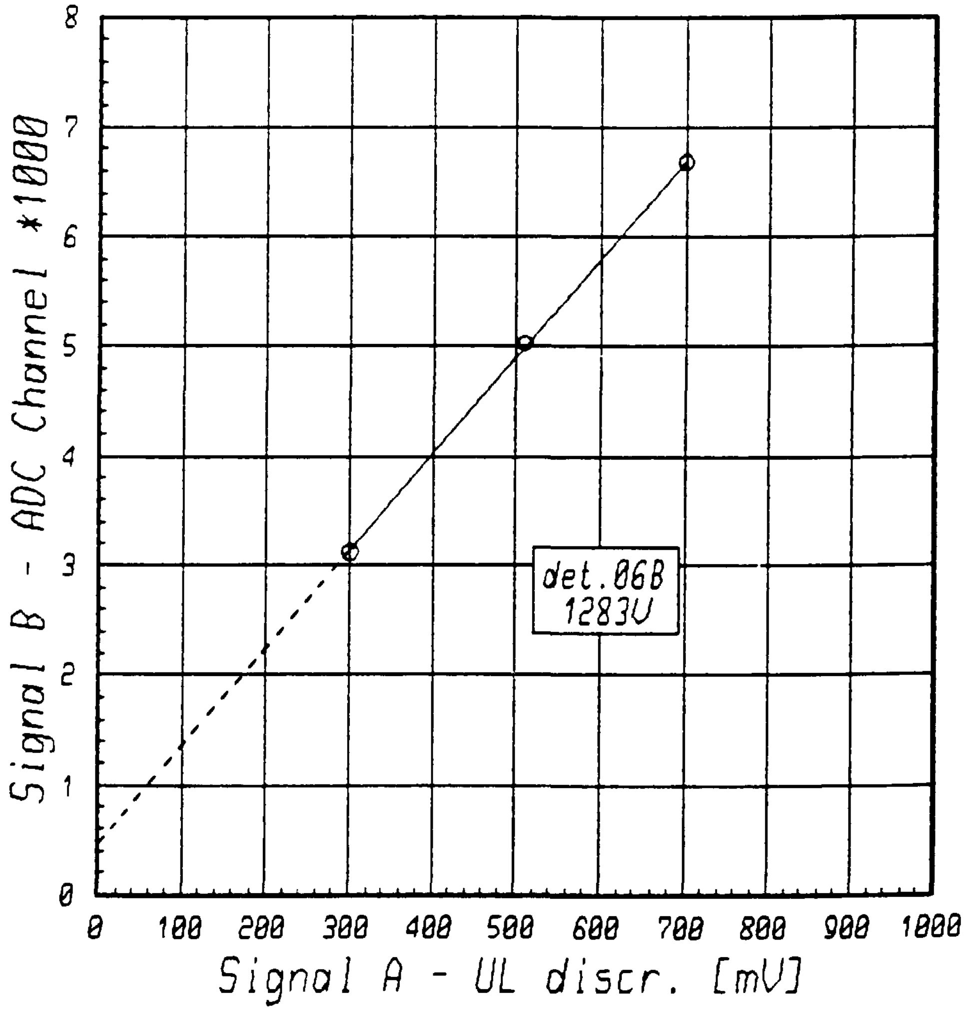

Fig.13 Position (channel) of the discrimination line in the distribution of linear signal B as a function of the discrimination level of fast signal A (Branch B, detector 06B, UL disc.iminator).

The dependence is described by the linear function

$$c = a \cdot D + a_0 \ , \qquad (6)$$

where

c is the position (channel) of the discrimination line observed in the distribution B,

D is the discrimination level of signal A, and

a, a_0 are constants.

One can fit the line Eq.(6) to experimental data and get the correction a_0 which should be introduced in adjustment of the discrimination level to the channel position. This procedure was performed for all the detectors chosen for the amplitude distribution indirect measurements. The results are given in Table 6. Then the energies (in the distribution B) corresponding to the discrimination levels of signal A were found. The results obtained for the same detectors and high voltages as listed in Table 6 are presented in Figs 14–18. Values for particular discrimination levels are given in Table 7. The calculated and "measured energies" seem not to coincide well. But if one refers the results for detectors 12B (two high voltages) and 00B to the corresponding plots (Figs 14–16) only a certain shift between the calculated and "measured" dependences A(E) is observed. We use here a quotation mark because the "measured" values are indirect and as it has been shown above (Figs 12, 13, and Table 6) they can be biased by a systematic error. This, of course, may also be the case of the values calculated from the determined calibration parameters. A little worse situation is observed for detector 06B where the calculated and measured lines A(E) are not parallel (Fig.17) although the difference at $D_L = 100$ mV is similar as for other detectors. For that detector we performed an additional measurement using the UL discriminator. Agreement of calculated and measured dependence A(E) is much better in this case (Fig.18).

Table 6. Corrections a_0 for the discrimination line position in the amplitude distributions of signal B.

Detector	High voltage (V)	Discr.	Parameters*) a (chan/mV)	a_0 (chan)	Experim. code
00B	1565	LL	3.789	116	H330
06B	1283	LL	4.408	102	H342
		UL	8.899	466	H342
12B	1447	LL	3.985	123	H329
	1425	LL	4.066	125	H336

*) a and a_0 are defined by Eq.(6)

Table 7. Comparison of the calculated and "measured" energies corresponding to chosen discrimination levels for several detectors.

Detector	High voltage (V)	Discr. (mV)	Energy calculated (keV)	Energy "measured" (keV)	Exp. code
00B	1565	150^L	100	116	H330A
06B	1283	150^L	100	119	H342
		700^U	1072	1039	H342F
12B	1447	150^L	100	117	H329A
	1425	150^L	124	137	H336G

L – LL discriminator

U – UL discriminator

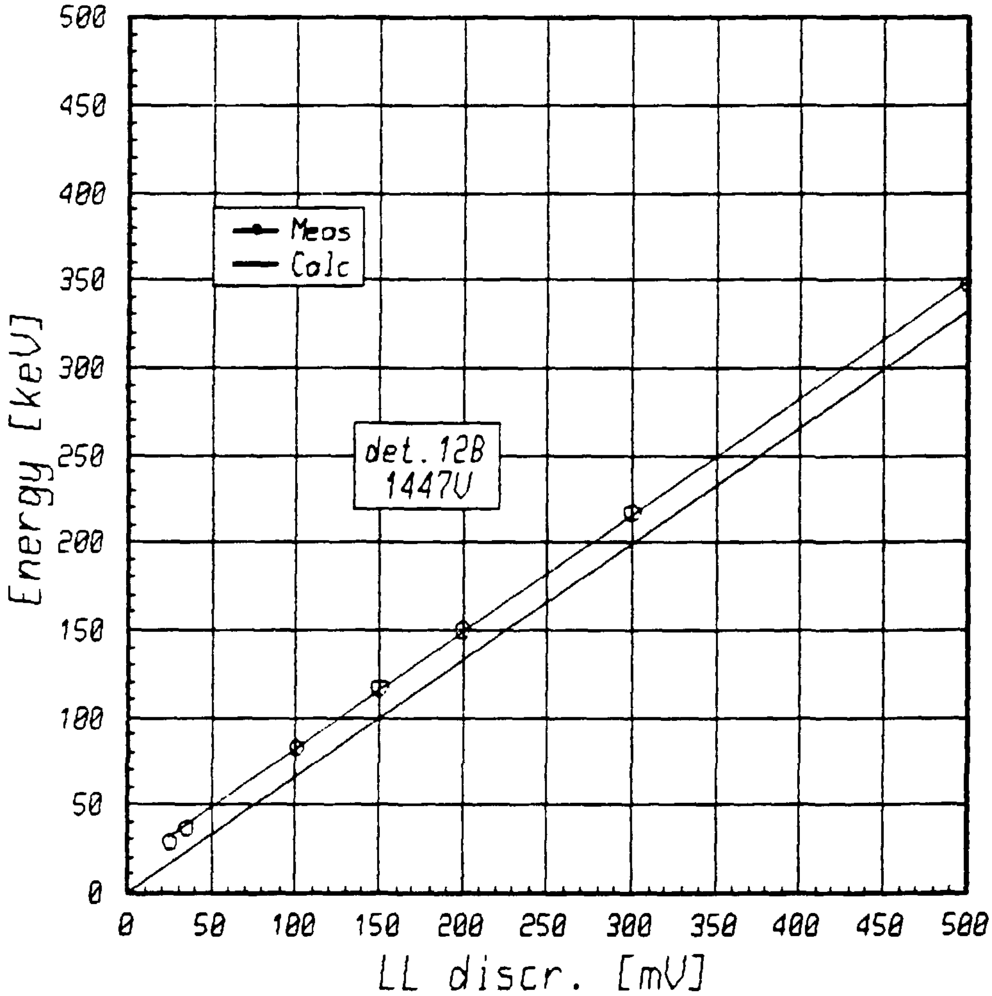

Fig.14. Calculated and "measured" correspondence of energy to discrimination level of fast signal A (detector 12B, high voltage 1447V, LL discriminator).

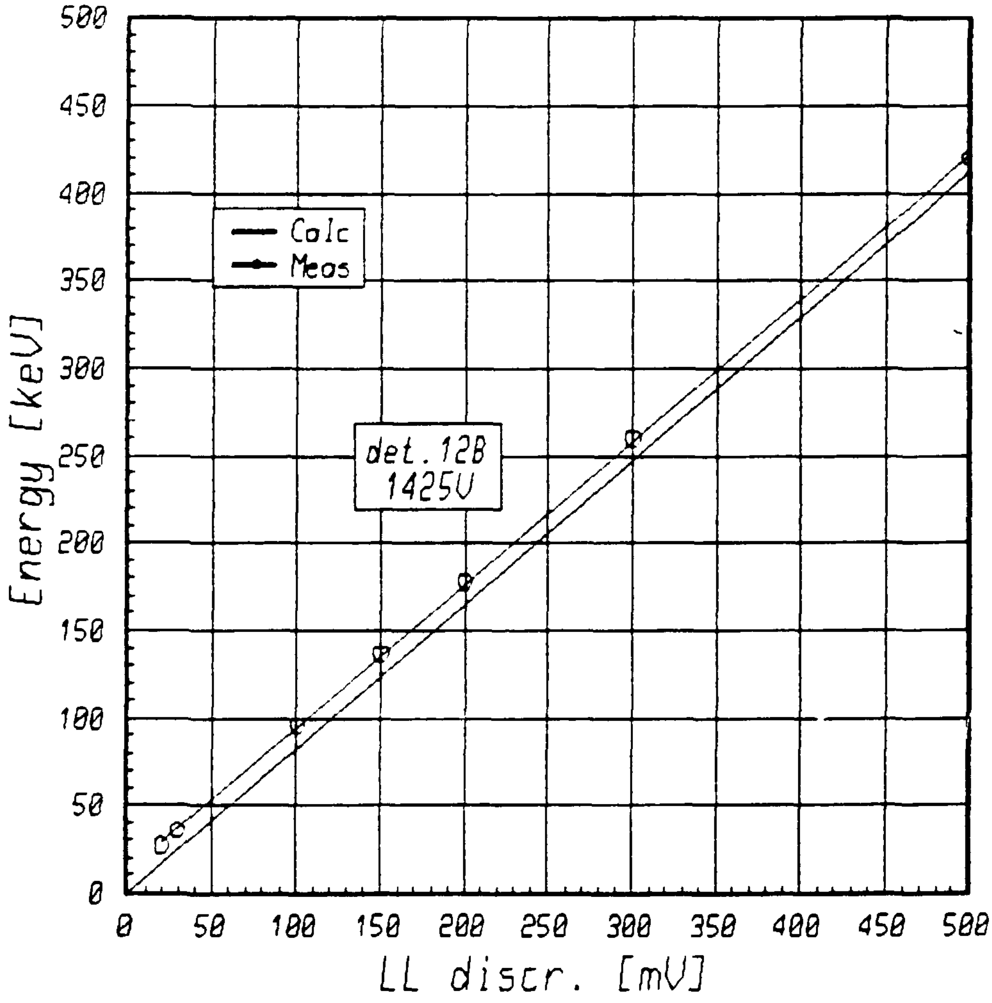

Fig.15. Calculated and "measured" correspondence of energy to discrimination level of fast signal A (detector 12B, high voltage 1425V, LL discriminator).

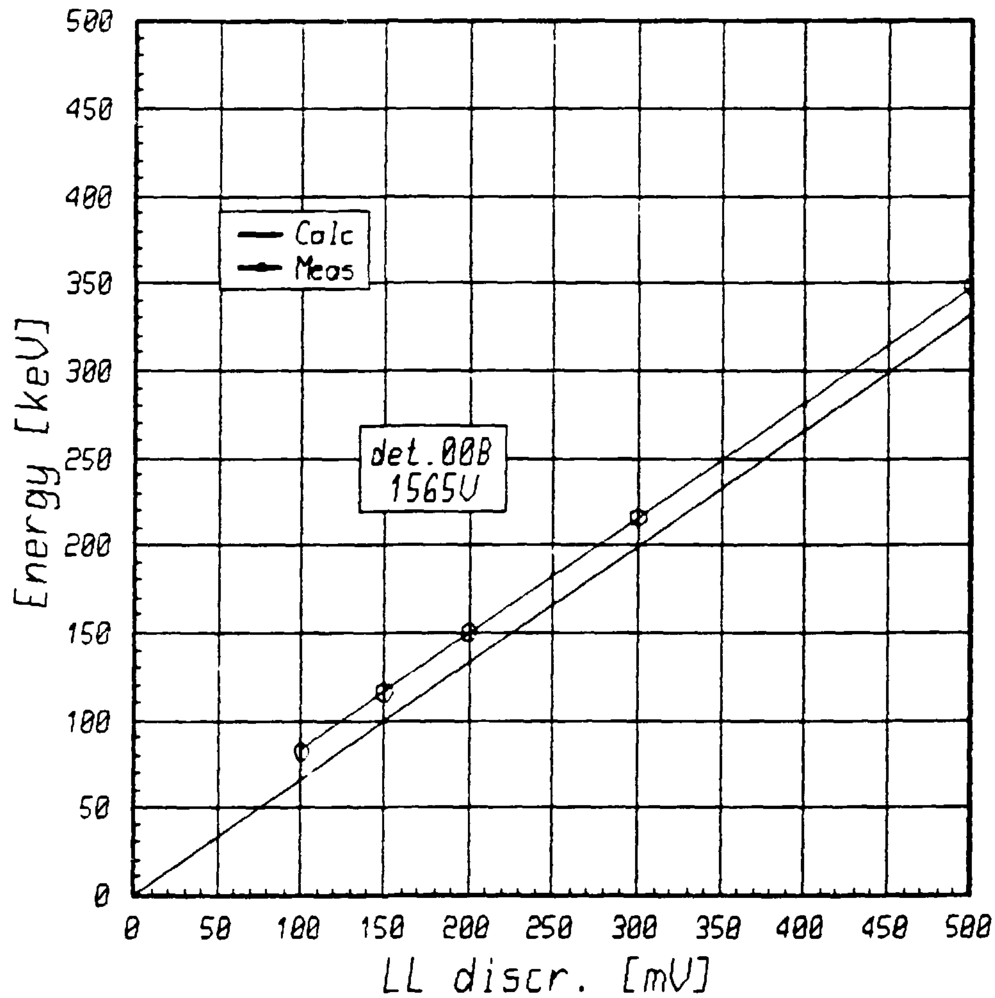

Fig.16. Calculated and "measured" correspondence of energy to discrimination level of fast signal A (detector 00B, high voltage 1565V, LL discriminator).

A conclusion from the test is that the determined calibration parameters of the neutron detectors can be influenced by a systematic error but the "measured" indirect values may as well. And the accuracy of these data is insufficient to be a base for any correction. Deviations of energies at $D_L = 150$ mV are smaller than the uncertainty of the discrimination line position observed in the energy distribution of signal B.

4.3. Test by Reference to a Source of Another Energy.

The calibration parameters of the TANSY neutron detectors were obtained from the measurements with the ^{60}Co source. We can check the parameters by calculating some values for another energy and compare them to measurement results at this energy. The check is done by doing the count rate distribution measurement for a certain discrimination level D using another γ source of a different energy. As usual, the peak position V_{Pm} of the differential distribution is found. Then it is compared to the calculated value V_{Pt} (based on Eq.(1)) for the i^{th} detector:

$$\ln(V_{Pt}) = \frac{1}{n_i} [\ln(D) - \ln(E_0'/E_0) - K_{0i}] \ , \tag{6}$$

where

E_0 is the ^{60}Co energy ,

E_0' is the energy of the used source, and

K_{0i}, n_i are the calibration parameters of the i^{th} detector .

The test measurements were performed using the ^{207}Bi source which gives two energy peaks of values $E_0' = 658 \pm 16$ keV and $E_0'' = 292 \pm 7$ keV (*cf* Table 5). Unfortunately, the source is much weaker than the used ^{60}Co source and it has to be placed closer to a detector (as in amplitude distribution measurements at 12.5 cm). Thus the count rate is sufficient to give reasonable statistics only for detectors in the neighbourhood of the chosen one. We used detector 12B for the measurement (see Fig.8) and we got also quite good data from eight others. The differential count rate distributions are plotted in Fig.19, and the calculated, V_{Pti}, and measured, V_{Pmi}, peak positions are compared in Table 8. The average deviations are: $\overline{V'_{Pti} - V'_{Pmi}} = +2.3V$ and $\overline{V''_{Pti} - V''_{Pmi}} = -3.4V$. They show that the values calculated from the determined calibration parameters and the ones measured in the test are in a very good statistical agreement. However, deviations of *ca* 10V are observed occasionally. Generally, in this experiment one can expect the deviations to be greater than 5V because now also the uncertainty in the determination of the energies E_0 is included. For ^{60}Co the $\sigma(E_0)$ is 27 keV and for ^{207}Bi $\sigma(E'_0)$ is 16 keV. In the measurement the uncertainty $\sigma(E_0) = 10$ keV makes the calculated peak position uncertain about 3V (it depends on the discrimination level, peak position, and values E_0). Our conclusion is that the obtained calibration parameters have been well confirmed.

Table 8. Calculated and measured peak positions in the differential count rate distributions for ^{207}Bi source ($E'_0 = 658$ keV, $E''_0 = 292$ keV) at discrimination level $D_L = 200$ mV.

Detector	V'_{Pt} calculated (V)	V'_{Pm} measured (V)	V''_{Pt} calculated (V)	V''_{Pm} measured (V)
03B	1250	1248	1327	1330
04B	1247	1250	1323	1326
05B	1345	1339	1426	1424
06B	1135	1137	1208	1216
10B	1257	1258	1333	≈ 1342
11B	1457	1446	1539	1544
12B	1290	1288	1368	≈ 1373
13B	1257	1247	1333	1327
14B	1238	1242	1314	1320

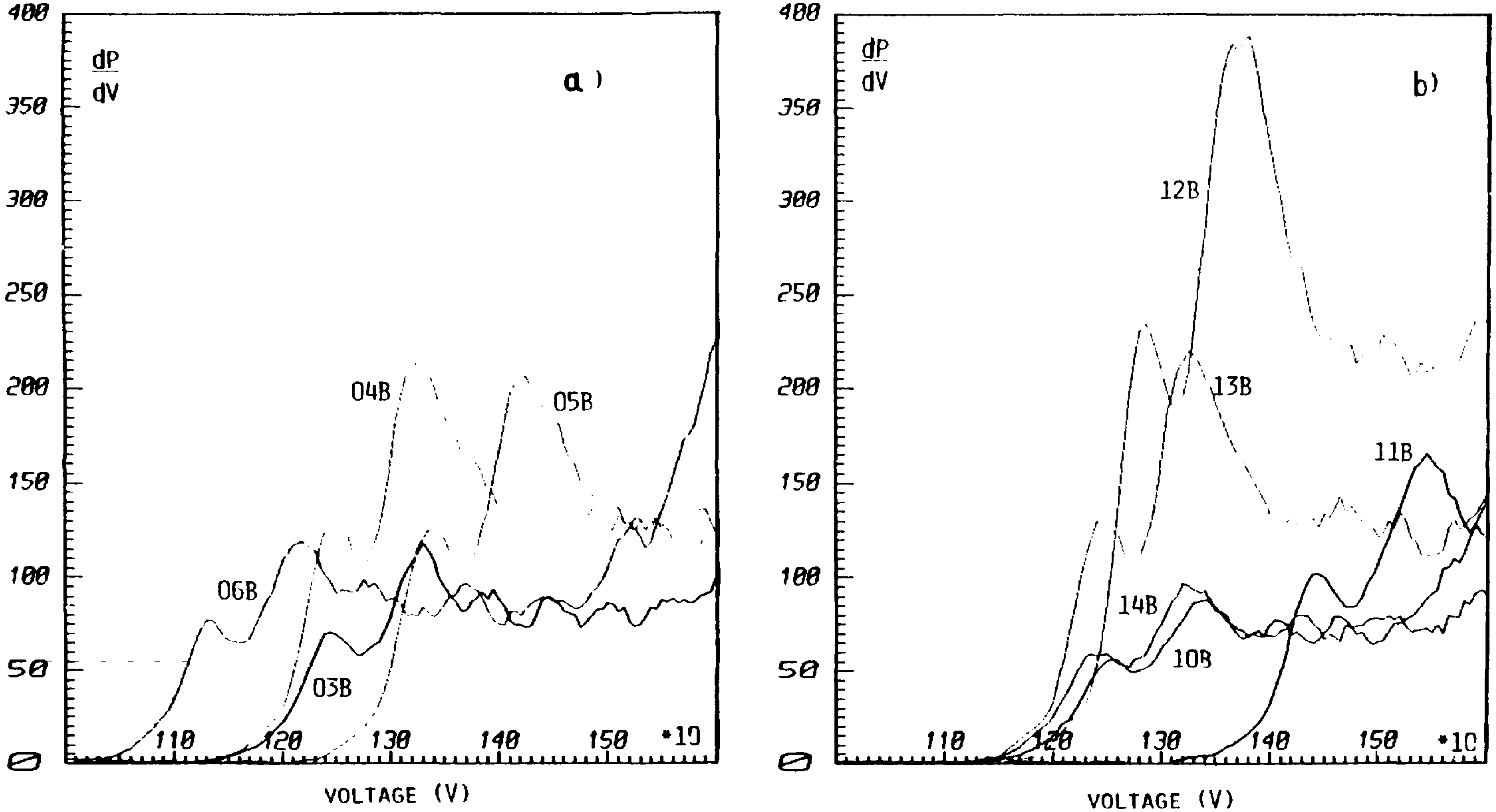

Fig.19. Differential count rate distributions dP/dV for a ^{207}Bi source placed in front of detector 12B. LL discriminator D_L = 200 mV. a) upper row detectors, b) lower row detectors, (*cf* Fig.8).

5. Long Time Stability of the Calibration

5.1. Verification of the Calibration Parameters

Small fluctuations in the discrimination and DC levels and in the voltages are all the time observed in the system. They cause fluctuations of the peak positions of the differential count rate distributions within 5V interval. But after some time has passed the amplification of the signal can change and then the calibration parameters do not fit the real situation. An experiment can be done to check such a long–time stability of the system. The experiment is precisely the same as done for the check of the calibration parameters immediately after the values are determined. Also now the calculated and measured peak positions in the differential count rate distribution are compared. If any differences are observed the calibration parameters should be corrected.

The experiments were done for all detectors in both branches A and B. Deviations greater than allowed by condition (5) were noticed only for two detectors in branch A and for one in branch B. Detector 11B was changed just before the calibration while others in branch B have been in function for a long time. This is probably a reason of the quite big shift of the present position of the peak. Therefore we did the measurement for branch B also at another discrimination level to check if the slope of the calibration line is preserved. The results are presented in Fig.20 (some detectors from branch A) and in Fig.21 (branch B).

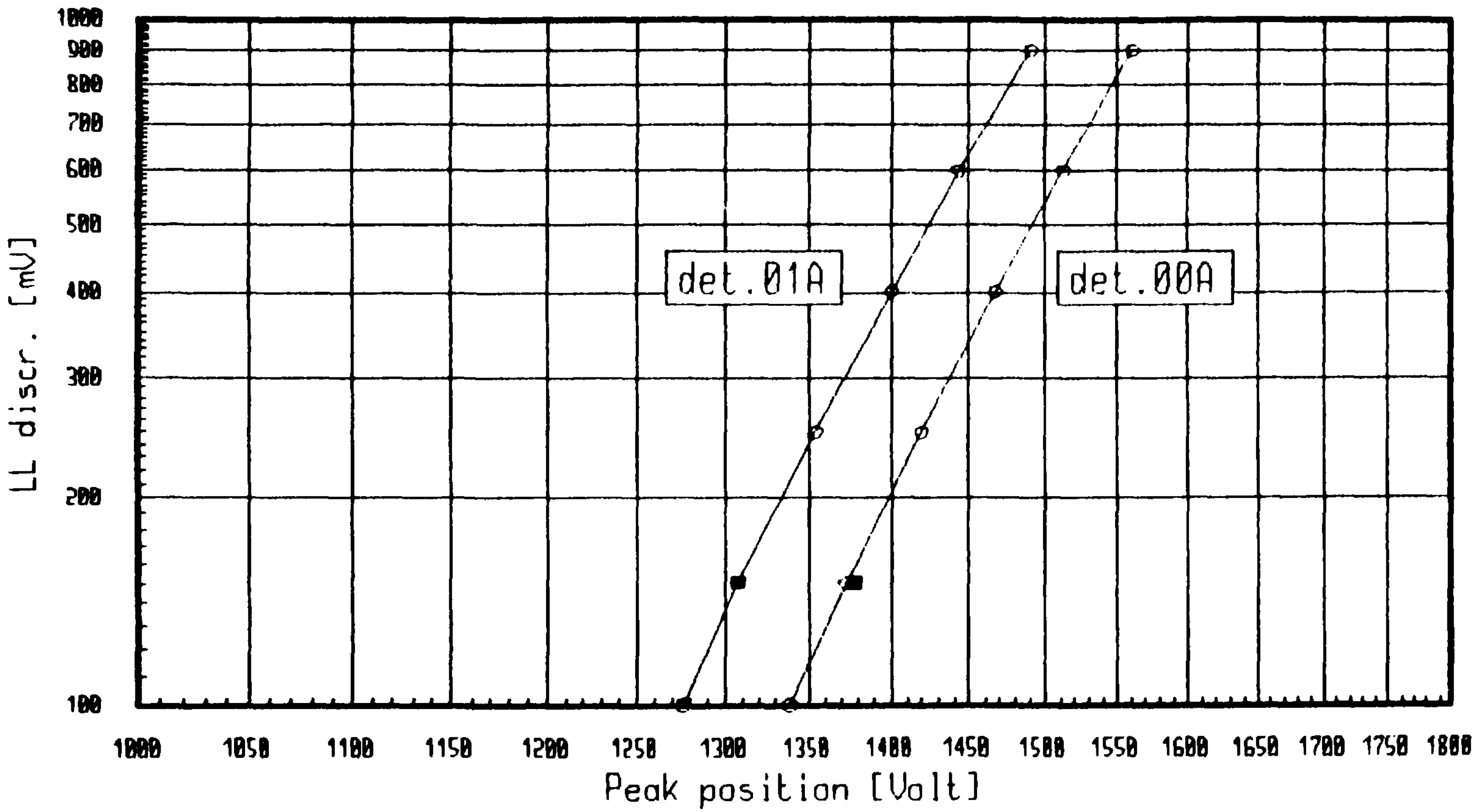

Fig.20a. Test of the long time stability of the calibration parameters. The verified positions $(V_P, D_L)_i$ are marked (•). Branch A, detectors 00A and 01A. A deviation for detector 00A is observed.

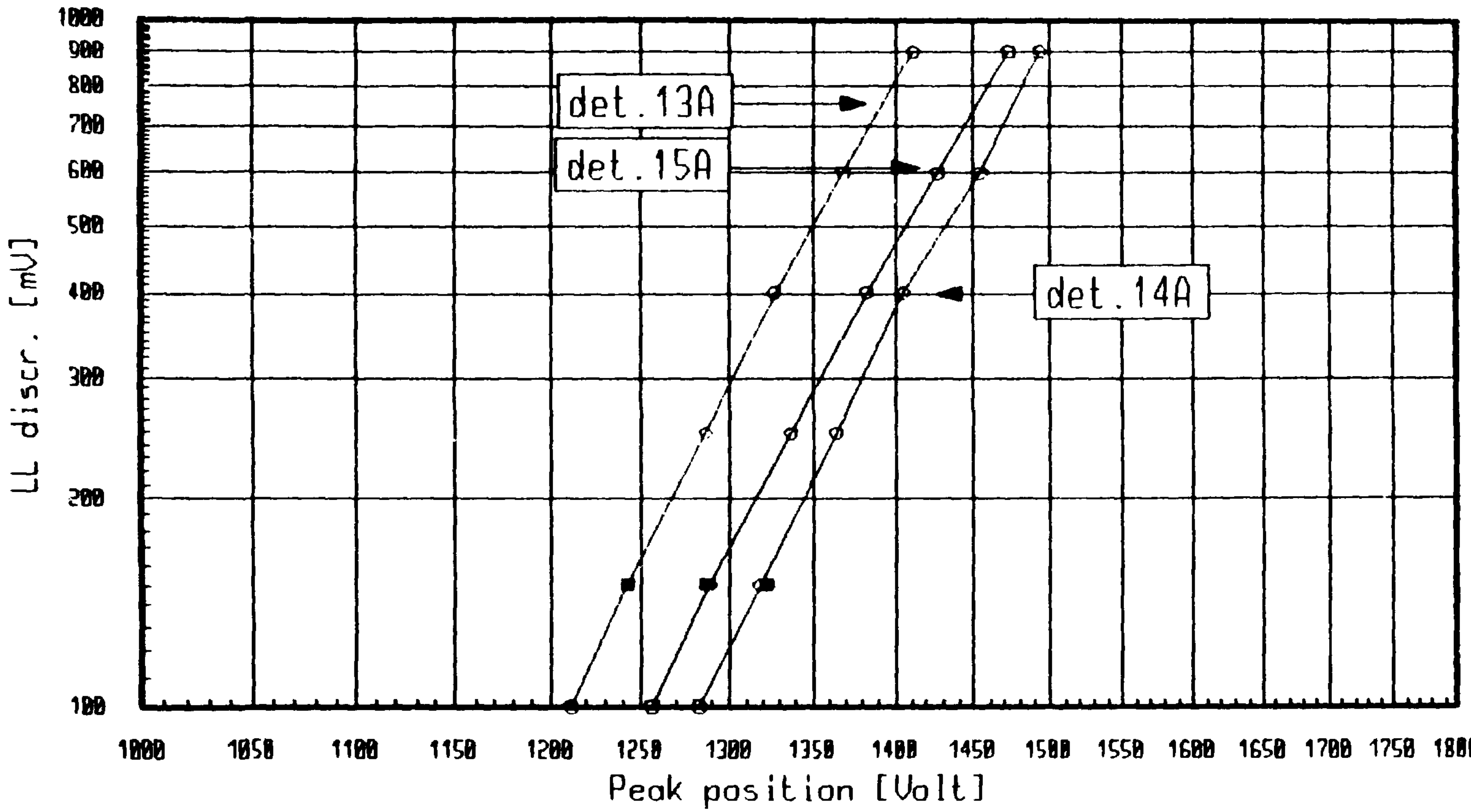

Fig.20b. Test of the long time stability of the calibration parameters. The verified positions $(V_P, D_L)_i$ are marked (▪). Branch A, detectors 13A – 15A. A deviation for detector 14A is observed.

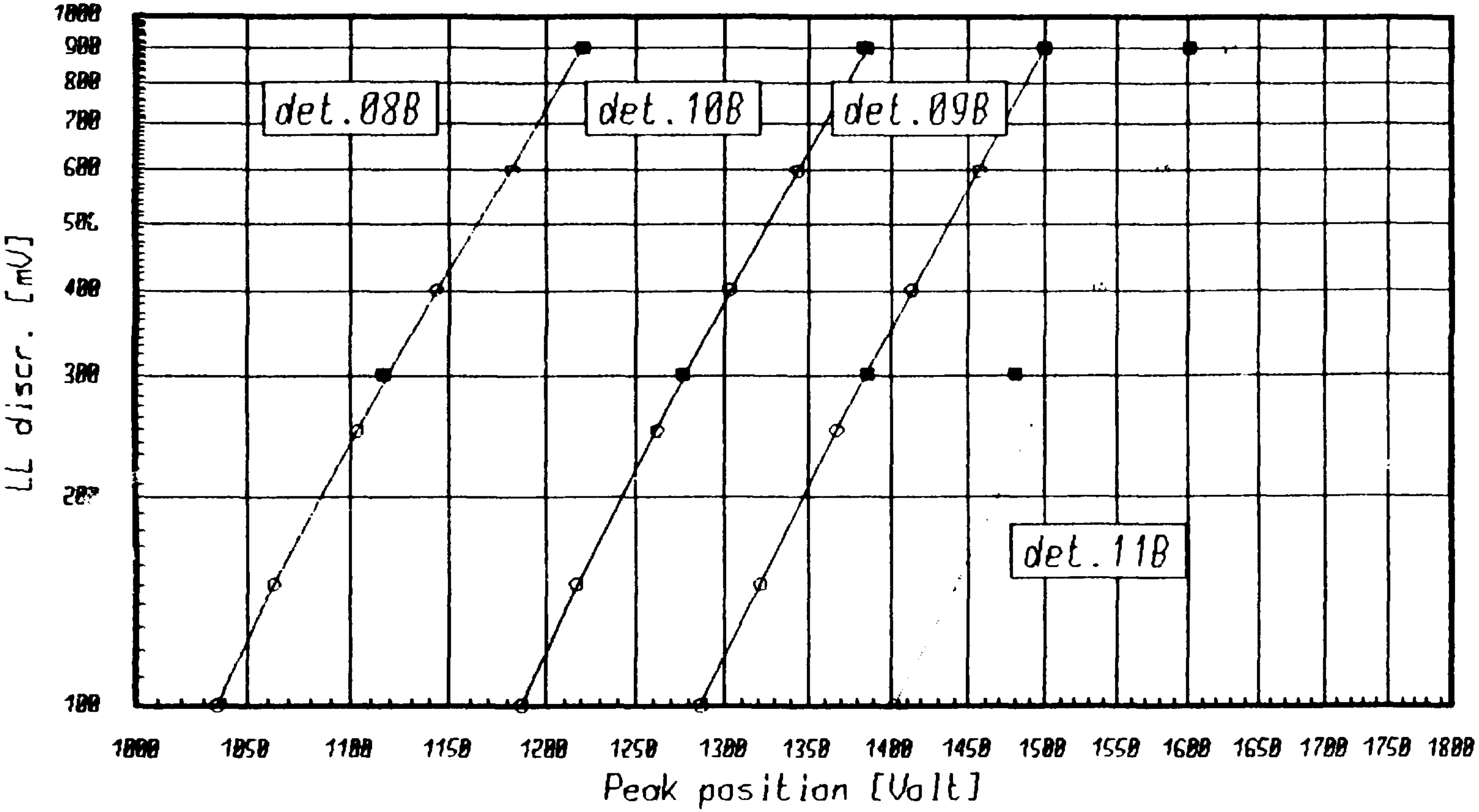

Fig.21. Test of the long time stability of the calibration parameters. The verified positions $(V_P, D_L)_i$ are marked (•). Branch B, detectors 08B – 11B. Deviations for detector 11B are observed.

The experiment for branch A was performed two times for the LL discriminators D_L = 150 mV :

i) when the UL discriminators were connected to the system as during the normal operation of the spectrometer, and

ii) when they were not used in the system, *ie* as it is during the normal calibration procedure.

The calculated peak positions , V_{Pti} , and the measured peak positions in the two cases, $V^{(1)}_{Pmi}$ and $V^{(0)}_{Pmi}$, are compared in Table 9. The measurement with the connected UL discriminators seems not to be fully correct. Detectors 01A and 05A show deviations for case *i*) but not for case *ii*), while detector 14A does not deviate for *i*) but does so for *ii*). This is because the presence of the UL discrimination disturbes the integral count rate distribution. It is no longer fully integral because from a certain high voltage a subtraction of the pulses which start to overcome the UL discrimination happens. (During normal operation the system works in anticoincidences $L \cdot \bar{U}$, where the logic signal L corresponds to $A > D_L$ and the signal U to $A > D_U$). This has been observed in the present experiment even for the low discrimination level D_L = 150 mV. Therefore the experiment has to be performed under the "calibration conditions" and not under the "operation conditions" when one really wishes to verify the calibration parameters, and perhaps to change them.

The results of the experiment for branch B at the LL discrimination D_L = 300 mV (while the UL discriminators were disconnected) are presented in Table 10.

Table 9. Results of the test of the calibration parameters after a long time (branch A, D_L = 150 mV).

Detector	Peak position (V)		
	calculated	measured	
	V_{Pt}	$V^{(1)}_{Pm}$	$V^{(0)}_{Pm}$
00A	1370.	1378.4	1377.0 (*)
01A	1305.	1311.0	1307.4
02A	1307.	1310.3	1307.0
03A	1301.	1303.0	1301.5
04A	1335.	1336.8	1332.9
05A	1352.	1357.5	1354.2
06A	1385.	1386.0	1382.4
07A	1388.	1392.1	1391.2
08A	1187.	1187.8	1187.4
09A	1248.	1247.7	1246.6
10A	1282.	1283.7	1282.4
11A	1285.	1286.9	1285.5
12A	1304.	1303.1	1301.4
13A	1240.	1242.4	1241.7
14A	1316.	1319.7	1322.6 (*)
15A	1287.	1287.9	1286.0

(1) with the UL discriminators in the system
(0) with no UL discrimination
(*) deviation greater than 5V

Table 10. Results of the test of the calibration parameters after a long time (branch B, D_L = 300 mV).

Detector	Peak position (V) calculated V_{Pt}	measured $V_{Pm}^{(0)}$
00B	1418.	1415.5
01B	1387.	1385.6
02B	1312.	1308.1
03B	1272.	1270.4
04B	1269.	1267.0
05B	1368.	1366.6
06B	1156.	1153.2
07B	1341.	1341.1
08B	1119.	1116.4
09B	1386.	1385.5
10B	1278.	1277.1
11B	1510.	1480.0 (*)
12B	1312.	1311.2
13B	1279.	1274.0
14B	1260.	1260.7
15B	1335.	1333.6

(0) with no UL discrimination
(*) deviation greater than 5V

5.2. Method to Update the Calibration Parameters.

During a long time of elaboration of the calibration method we noticed that the parameters n_i are stable. The behaviour was also confirmed in the last measurement, even in the case of such a big change as for detector 12B, *cf* Fig.21. This offers us a very simple method of updating the calibration parameters. For each detector we have the following data:

K_{0Li}, n_{Li}, K_{0Ui}, n_{Ui} — old calibration parameters
D_L — LL discrimination at which the count rate distribution has just been measured
V_{Pmi} — measured peak position
V_{Pti} — peak position calculated from the old parameters.

If the difference between the calculated and measured peak position exceeds the permissable level ΔV_P (*cf* condition (5)) the updated values of the calibration parameters should be found: K^x_{0Li}, n^x_{Li}, K^x_{0Ui}, n^x_{Ui}. The n_i parameters are not changed:

$$n^x_{Li} = n_{Li} \ , \tag{7a}$$

$$n^x_{Ui} = n_{Ui} \ . \tag{7b}$$

From Eq.(2) the updated parameter K^x_{0Li} can be calculated

$$K^x_{0Li} = \ln(D_L) - n_{Li} \cdot \ln(V_{Pmi}) \ , \tag{8}$$

where the new measured position of the peak V_{Pmi} is utilized.

The new value of the parameter K^x_{0Ui} can be found as follows. Generally, the parameter K_0 is related to a coefficient C_0 proportional to an amplification (not including the PM–tube gain) in the following way:

$$A = C_0 \cdot V^n , \tag{9}$$

$$K_0 = \ln(C_0) \tag{10}$$

(*cf* Eqs (4), (6), (8) in [1]) . Input signal for the UL discriminator is in fact the same signal as for the LL but it has been attenuated in the system. That means that the relation between the amplification coefficients for the LL and UL discriminators is constant:

$$\frac{C^x_{0Ui}}{C^x_{0Li}} = \frac{C_{0Ui}}{C_{0Li}} , \tag{11}$$

which with Eq.(10) gives the new calibration coefficient for the upper level:

$$K^x_{0Ui} = K_{0Ui} + (K^x_{0Li} - K_{0Li}) . \tag{12}$$

The change of the parameters is based on a result of only one measurement. Therefore all the conditions have to be checked carefully before running that experiment. The DC levels of the output signals from the PM–bases have to be set to zero, the discrimination levels D_L have to be set very accurately, and the UL discriminators have to be disconnected from the system.

6. Correlation Between the Neutron Detector Calibration Parameters and the Producer's Data for the Photomultipliers.

The producer*) of the photomultipliers gives some parameters of each PM–tube. For example, a monochromatic sensitivity is given and a voltage corresponding to a certain fixed gain of the tube. The parameters are measured in factory standard test conditions. In our operation conditions the amplitude of the signal is analysed and not the PM–tube current, and also the PM–base was included, which influences the output signal. However, we tried to investigate a dependence between the producer's data and our calibration parameters.

The output pulse amplitude A can be written as:

$$A \sim S_1 \cdot S_2 \cdot S_3 \cdot S_4 \qquad (13)$$

where

S_1 is the coefficient of the quality of the optical coupling ,

S_2 is the light sensitivity of the PM ,

S_3 is the gain of the PM, and

S_4 is the amplification in the PM–base .

We may assume the same value of the coefficient S_1 for all detectors in our two arrays

$$S_{1i} = S_1 = \text{const} \ , \qquad (14)$$

because they were prepared in the same manner and under the same conditions.

*) Philips, Electronic Components and Materials

The light sensitivity, S_2 , should be proportional to the parameter S_M given by the producer:

$$S_2 \sim S_M \ , \tag{15}$$

where S_M is the monochromatic sensitivity for the 401 nm wavelength, expressed by the PM current per unit power of the light source.

The PM gain was given by Eq.(2) in [1]:

$$S_3 = k \cdot V^n \ . \tag{16}$$

The producer reports the high voltage value V_{PH} at which the photomultiplier reaches a standard gain $S_3 = S_S$ ($3 \cdot 10^7$ in this case of the PM type XP2041). Thus we have:

$$S_S = k \cdot V^n_{PH} \tag{16a}$$

and

$$S_3 = S_S \cdot V^n / V^n_{PH} \tag{16b}$$

Finally, the amplitude A is described, using Eqs (14), (15) and (16b), by the dependence:

$$A \sim S_4 \cdot S_M \cdot V^n / V^n_{PH} \ . \tag{17}$$

The same amplitude is given by Eq.(9). The comparison yields

$$C_0 = S_4 \cdot S_M / V^n_{PH} \ . \tag{18}$$

The coefficient S_4, which characterizes the PM–base, is unknown. It is not exactly the same for various bases and can change for one base depending on some adjustments (focusing procedure). That means that for one particular detector we still have the proportionality:

$$C_0 \sim S_M / V_{PH}^n , \tag{19}$$

but generally for all detectors together the dependence (19) can be fulfilled only in statistical sense

$$C_{0i} \mathrel{\hat{\sim}} S_{Mi} / (V_{PHi})^{n_i} \qquad i = 0,...,I \tag{20}$$

if we assume not very differing PM–bases:

$$S_{4i} \approx S_{4k} . \tag{21}$$

From Eq.(20) we get a direct dependence between the calibration parameters and the producer's data:

$$K_{0i} \mathrel{\hat{\sim}} \ln(S_{0i}) + \text{const} , \tag{22}$$

where

$$S_{0i} = S_{Mi} / (V_{PH})^{n_i} . \tag{23}$$

The combined parameter S_0 was calculated for each detector (with one exception: we do not have producer's data for detector 06B). The producer's values of S_M and V_{PH} for selected detectors are listed in Table 11 to show some average and extreme data.

Table 11. Producer's data for selected PM–tubes.

Detector	PM No.	S_M (mA/W)	V_{PH} (V)
11B	13180 E9A	69	2180
15A	12912 E7H	73	2060
04A	12953 E7J	82	2140
05B	12997 E7K	83 *)	2080
08B	13013 E7K	86	1790
03A	12952 E7L	92	2090
10B	13015 E7K	95	1810

*) Average value

The parameters K_0 and n are taken from the final results (after verification) of the calibration for LL discriminators, see Tables 13 and 14. The pairs $(K_0 , \ln(S_0))_i$ are plotted in Fig.22 for detectors of branch A, and in Fig.23 for detectors of branch B. The linear regression gave high correlation and practically the same straight line in both cases. The results are shown in Table 12, and all the data (branches A and B together) are plotted in Fig.24.

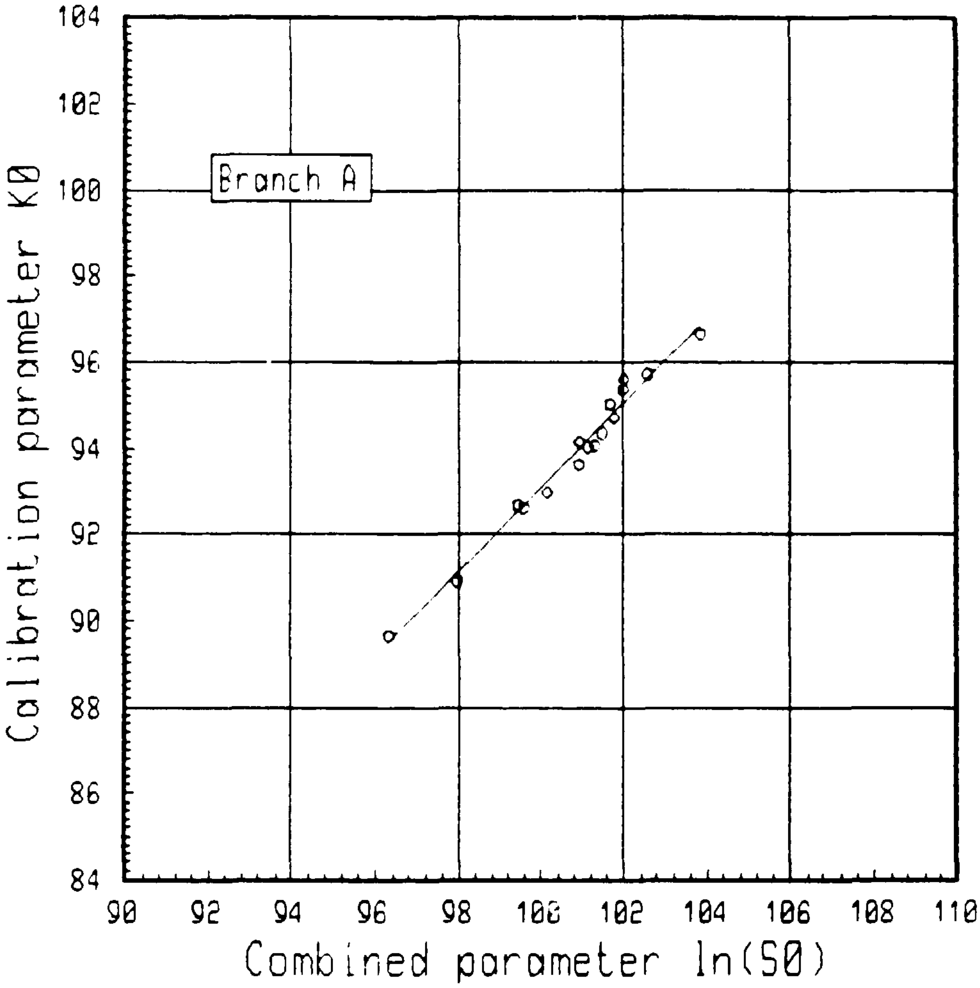

Fig.22. Correlation between the calibration parameters of the TANSY neutron detectors and the producer's data for the used photomultipliers (detectors of branch A).

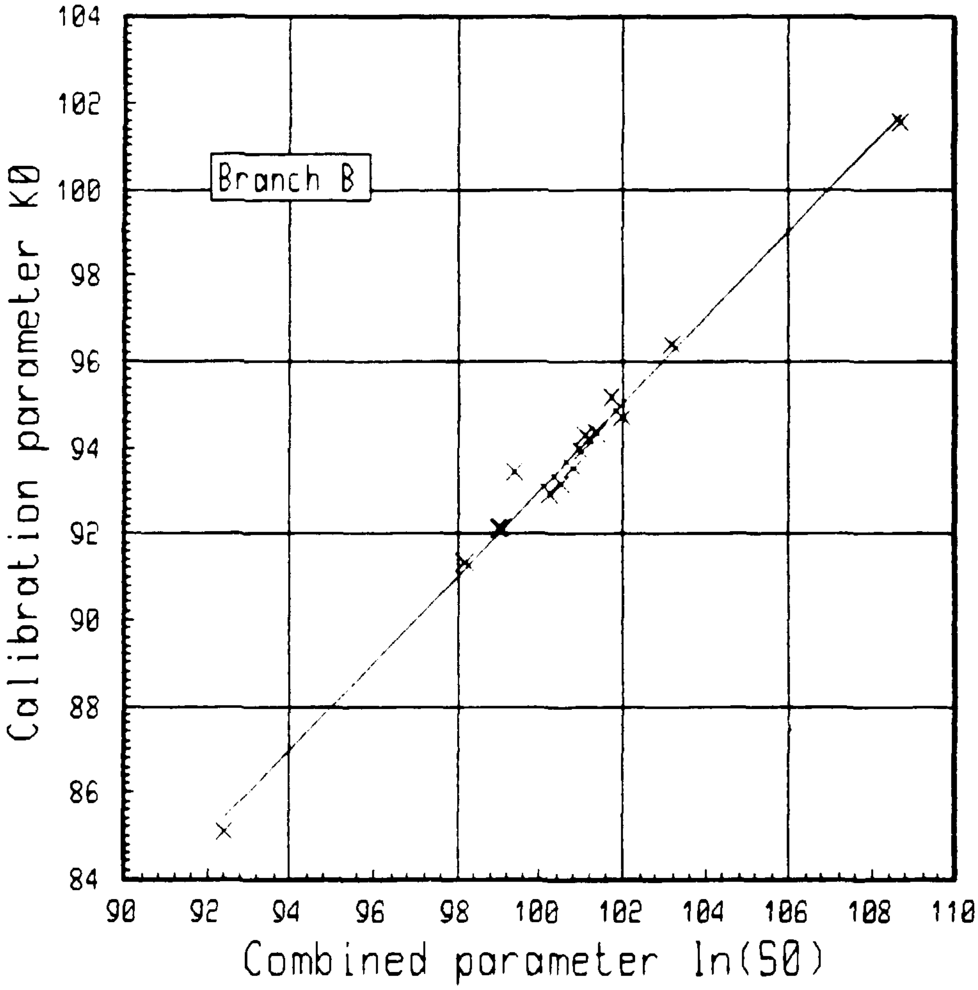

Fig.23. Correlation between the calibration parameters of the TANSY neutron detectors and the producer's data for the used photomultipliers (detectors of branch B).

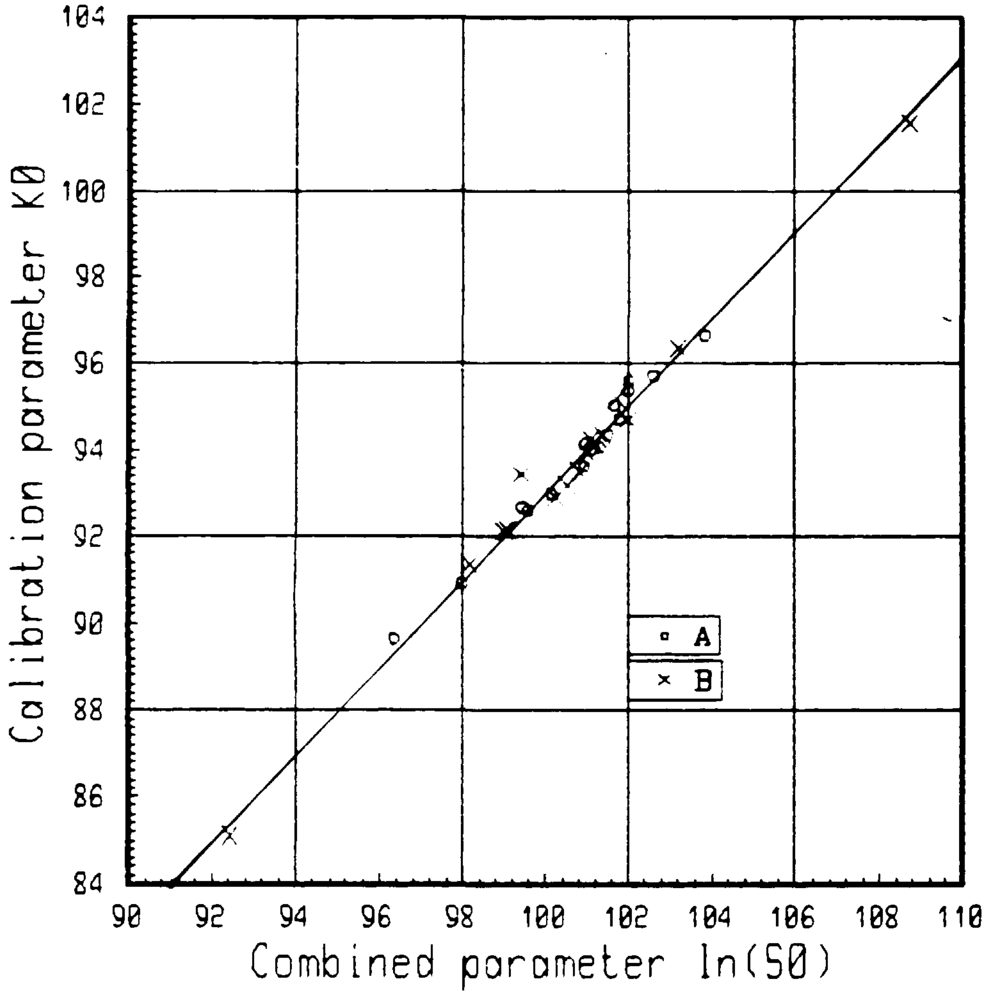

Fig.24. Correlation between the calibration parameters of the TANSY neutron detectors and the producer's data for the used photomultipliers (detectors of branch A and B).

Table 12. Correlation between the calibration parameters and producer's data: $K_0 = m \cdot \ln(S_0) + m_0$.

	Detectors of branch A	B	A+B
m	0.9811	1.0203	0.9962
m_0	–5.0436	–8.9882	–6.5711
$\rho(K_0, \ln S_0)$	0.9901	0.9897	0.9929

The conclusion is that there is a very high correlation between the producer's data and the measured calibration parameters for the neutron detectors. However, the dependence is statistical (because of some unknown factors) and does not allow us to calculate exact values of the parameters for the calibration in an individual case. The precision of the V_{PH} data (ca 10V) seems also to be insufficient.

7. Conclusions

7.1. General Conclusions

The elaborated method described in this report and in [1] seems to be relevant to make a calibration of the TANSY neutron detectors. The method offers the user the simplest way to simultaneously determine the calibration parameters for all the detectors in an array. The experiment, although it may be laborious, needs much less measurements then any calibration done by classic amplitude distributions for each detector. An important advantage of the method is that the same equipment is used for this calibration as for normal operation of the spectrometer. Therefore, later tests are easy to perform.

The test measurements performed to check the method and the values of the calibration parameters show very good internal consistency of the method. The calibration parameters have also been confirmed by (statistical) relation to the producer's data for the photomultipliers. However, a small systematic error cannot be excluded (*eg* due to a non–linearity at very low energies which were not possible to investigate). We noticed a discrepancy between the energy dependences calculated for the detectors, based on the obtained calibration parameters, and energies measured by the indirect amplitude distribution for several detectors. Due to a significant uncertainty of the data from these distributions we may only state that there may be a difference between the results of the two methods. We are even not sure of the existence of that difference because it is less than the uncertainty of the energy values (*cf* paragraph 4.2). Furthermore there is no indication which of the two experiments that is the better one. The final conclusion is that the determined calibration parameters should give an energy deviation not larger than *ca* 15 keV (electron energy) at the LL discrimination D_L = 150 mV. A deviation in the UL discrimination is generally of less importance and even if the deviation is about twice as large it corresponds to only about 2%. Therefore the obtained calibration parameters can be used for calculation of the settings for the TANSY neutron detectors.

7.2. Settings for the TANSY Neutron Detectors.

The settings for the detectors include the operation high voltages and the LL and UL discriminations. They should correspond to the lower and upper energy levels required by the user.

A method to obtain the settings has been shown in Fig.12 in [1]. The procedure is as follows:

1) assume the LL discrimination, D_L, for all detectors ,
2) assume the LL energy, E_L, for all detectors ,
3) calculate the individual operation high voltages, V_i, from Eq.(1) using the input data: $E_0 = E_0(^{60}Co)$, $E = E_L$, $A = D_L$, $n = n_{Li}$, $K_0 = K_{0Li}$,
4) assume the UL energy, E_U, for all detectors , and
5) calculate the individual UL discriminations, $D_{Ui} = A$, from Eq.(1) using the input data: $E_0 = E_0(^{60}Co)$, $E = E_U$, $V = V_i$, $n = n_{Ui}$, $K_0 = K_{0Ui}$.

The following requirements are presumed for the TANSY neutron detectors: $D_L = 150$ mV, $E_L = 100$ keV, $E_U = 1400$ keV (electron energies). The reference to the neutron energy has been given in [1] according to [6]. The corresponding settings are listed in Table 13 (branch A) and Table 14 (branch B) together with the final values of the neutron detector calibration parameters which were obtained when the verification tests were done.

Table 13. Final values of the calibration parameters and settings for the TANSY neutron detectors, branch A (09–MAY–90).

SETTINGS for energy-calibrated NEUTRON DETECTORS - branch A.

Input data:
LL Energy = 100.0 [keV]   LL Discrim. = 150.0 [mV]
UL Energy = 1400.0 [keV]

Calibration parameters:

E0 = 781.0 [keV] - Co-60 Energy

Neutron detector parameters: VERSION 1 of 09-MAY-90

det#A	LL LN(C)	LL n	UL LN(C)	UL n
00	-95.59770	13.9199	-95.93807	13.8552
01	-92.98448	13.6593	-97.03045	14.1008
02	-92.67700	13.6140	-94.83014	13.7963
03	-94.71216	13.9067	-96.51661	14.0441
04	-94.02595	13.7617	-94.33855	13.6972
05	-94.15124	13.7548	-93.86630	13.6082
06	-95.71883	13.9254	-93.99732	13.5837
07	-95.37336	13.8737	-97.10278	14.0017
08	-89.64796	13.3720	-92.16994	13.6088
09	-94.05767	13.8962	-92.76257	13.6038
10	-92.60953	13.6415	-92.78299	13.5531
11	-93.63454	13.7802	-94.57716	13.7974
12	-94.35622	13.8519	-97.09632	14.1143
13	-95.02723	14.0444	-95.59081	14.0087
14	-96.64515	14.1437	-98.74255	14.3156
15	-90.92054	13.3984	-92.85490	13.5530

SETTINGS FOR NEUTRON DETECTORS - BRANCH A.
===

det#A	LL discr. [mV]	UL discr. [mV]	HV [V]
00	150.	927.	1596.
01	150.	932.	1517.
02	150.	927.	1520.
03	150.	945.	1508.
04	150.	957.	1550.
05	150.	949.	1570.
06	150.	943.	1605.
07	150.	959.	1610.
08	150.	935.	1384.
09	150.	913.	1447.
10	150.	925.	1490.
11	150.	928.	1492.
12	150.	926.	1513.
13	150.	922.	1436.
14	150.	909.	1529.
15	150.	940.	1500.

Table 14. Final values of the calibration parameters and settings for the TANSY neutron detectors, branch B (27–APR–90).

```
SETTINGS for energy-calibrated NEUTRON DETECTORS - branch B.

Input data:
          LL Energy =  100.0 [keV]    LL Discrim. =  150.0 [mV]
          UL Energy = 1400.0 [keV]

Calibration parameters:

          E0 =  781.0 [keV]    -  Co-60  Energy

     Neutron detector parameters:    VERSION 1   of 27-APR-90
```

det#B	LL LN(C)	LL n	UL LN(C)	UL n
00	-94.32612	13.7845	-97.53858	14.1077
01	-94.69771	13.8778	-96.95764	14.0739
02	-95.20302	14.0554	-93.84972	13.7565
03	-91.35313	13.5781	-94.32944	13.8779
04	-93.16808	13.8366	-94.18201	13.8629
05	-93.91614	13.7961	-96.26985	14.0069
06	-85.90939	12.9904	-85.23893	12.7811
07	-92.92239	13.6960	-92.48105	13.5235
08	-85.10455	12.9348	-80.74310	12.2098
09	-96.38091	14.1114	-97.91914	14.2092
10	-93.43744	13.8595	-91.37764	13.4656
11	-101.54265	14.6917	-106.64184	15.2696
12	-94.26544	13.9245	-94.83786	13.8927
13	-93.53030	13.8722	-93.36443	13.7377
14	-92.13696	13.7060	-93.20802	13.7402
15	-92.13000	13.5939	-94.02959	13.7413

SETTINGS FOR NEUTRON DETECTORS - BRANCH B.
===

det#B	LL discr. [mV]	UL discr. [mV]	HV [V]
00	150.	911.	1565.
01	150.	923.	1530.
02	150.	923.	1445.
03	150.	941.	1406.
04	150.	922.	1400.
05	150.	934.	1510.
06	150.	918.	1283.
07	150.	927.	1481.
08	150.	939.	1244.
09	150.	924.	1527.
10	150.	947.	1410.
11	150.	918.	1624.
12	150.	940.	1447.
13	150.	935.	1410.
14	150.	922.	1391.
15	150.	921.	1476.

7.3. Tests of the TANSY Neutron Detectors Settings During Operation of the Spectrometer.

Two types of tests are proposed. The first one is a background test to be run *eg* every week. It should detect any change of the settings which gives a significant deviation of the pulse amplitude window. At the same time it should allow the usual observed fluctuations in the system. The test is called "passive test".

The second test, "active test", should be run when the results of the passive test are unsatisfactory. It should indicate if the calibration parameters are to be updated and should give the new values if necessary.

Both the tests are based on the count rate distribution measurement.

7.3.1. Passive Test

The test is thought to be possible with the smallest effort and smallest changes (if any) in the operating system. The count rate distribution measurement is performed at the usual LL discrimination, D_L = 150 mV, (no adjustment) and the UL discriminators remain connected to the electronic system. The count rate divider has to be preset to 1. The ^{60}Co source (the same as during the calibration) is used. It is recommended to place the source in the centre of the foil–position in the vacuum vessel. An outside position is permitted but it can introduce a small shift in peak positions and should be avoided if possible.

The peak positions V_{Pmi} of the differential count rate distributions are determined and compared to the calculated ones, V_{Pti}, *cf* paragraph 4.1.

The test gives a positive result if all the detectors fulfil condition (5) with ΔV_P = 7V. The allowed difference ΔV_P is increased here because an additional shift is included by the presence of the UL discriminators.

A negative result of the test means that either the fluctuations of the DC and/or discrimination levels deviate from preset values or that the neutron detector calibration parameters have changed in time. In this case the active test has to be run.

7.3.2. Active Test (Updating the Calibration Parameters)

The active test is also reduced to only one single count rate distribution measurement but performed in conditions preseıved very rigorously. The order of the items given below should be strictly followed.

i) Adjust the DC levels of the output fast signal from all PM–bases to 0.0 ± 0.4 mV (measured with a 50Ω termination on the second output while the first one has to be connected to the LL discriminator).

ii) Preset all the LL discriminators to the same value $D_L \pm 1$ mV (D_L = 150 mV is recommended, but $150 \text{ mV} \le D_L \le 300 \text{ mV}$ can be used) .

iii) The UL discriminators have to be disconnected from the input to the coincidence unit, still obeying the condition $L \cdot \overline{U}$.

iv) The ^{60}Co source has to be placed in the centre of the vacuum vessel.

v) Run the count rate distribution measurement.

An analysis of the experiment gives the answer whether the peak positions fulfil condition (5) with $\Delta V_P = 5V$. It can occur in spite of a bad result of the passive test because all the adjustments have been improved and the reason for any deviations could have disappeared. If the peak positions deviate more than 5V then the status of the electronic system has changed. A change in the amplification of the signal chain, including the PM–tubes, is most probable. The procedure of updating the neutron detector calibration parameters has to be done as shown in paragraph 5.2. Then a new file of the calibration parameters is created which is used by those computer programs which are related to the energy calibration of the TANSY neutron detectors.

7.4. A Method to Apply a Spare Neutron Detector in the Array.

The calibration procedure should be performed for any new detector which is to be used in the neutron detector array. However, it is quite laborious and time consuming and special conditions have to be fulfilled. Therefore it is convenient to have a method which allows the user to quickly apply a new detector with approximate values of the parameters. Such a method is based on the observation that the calibration lines are almost parallel for all the detectors. One can assume that for a new detector n the calibration parameter n_n is:

$$n_{Ln} = \bar{n}_{L(AB)} \tag{24a}$$

$$n_{Un} = \bar{n}_{U(AB)} \tag{24b}$$

where the means $\bar{n}_{L(AB)}$ and $\bar{n}_{U(AB)}$ are calculated from an average of the values in branches A and B. Then the count rate distribution is measured at the LL discrimination $D_L = 150$ mV in the same rigorous conditions as in the active test (paragraph 7.3.2.). When the peak position V_{Pn} of the differential distribution is found the K_0 parameter is calculated from:

$$K_{0Ln} = \ln(D_L) - n_{Ln} \cdot \ln(V_{Pn}) \tag{25}$$

(*cf* Eq.(8)). The parameter K_0 for the UL discriminator can be found from the relation:

$$K_{0Un} \approx K_{0Ui} + (K_{0Ln} - K_{0Li}) \ , \tag{26}$$

where K_{0Li} and K_{0Ui} are the parameters of the detector which is now substituted by the new detector. Eq.(26) was obtained similarly as Eq.(12).

The method gives good parameters as a base for calculating the detector settings (D_L, E_L, V_n, E_U, D_{Un}) at the discrimination level at which the count rate distribution was measured. However, if for some reason significantly different values of the LL discrimination and/or the values of the lower and upper discrimination energies are wanted, then the approximated calibration parameters, n_{Ln} , n_{Un} , K_{0Ln} and K_{0Un} , may lead to unacceptable (and unknown) errors. In this case one should perform the full calibration procedure (as described in paragraph 2) for the new detector to get the true calibration parameters as quickly as possible.

Acknowledgement

We are indebted to Dr. G. Grosshög for the introduction and encouragement of the subject of this paper. We are grateful for his many useful suggestions and good advice during the course of the work.

References

[1] M. Hök, K. Drozdowicz and D. Aronsson: *Method of Energy Calibration of the TANSY Neutron Detectors.* Report CTH–RF–68, Göteborg (1990)

[2] G. Grosshög, D. Aronsson, E. Arvidsson, K.-H. Beimer, L.O. Pekkari, R. Rydz and N.G. Sjöstrand: *Combined Proton - Recoil and Neutron Time - of - Flight Spectrometer for 14 MeV Neutrons.* Report CTH–RF–43, 2nd ed., JET–JB2–9008, Göteborg (1983)

[3] G. Grosshög, D. Aronsson, K.-H. Beimer, L.O. Pekkari, R. Rydz, Ö. Skeppstedt and N.G. Sjöstrand: *TANSY a Neutron - Spectrometer for Fusion - Plasma Diagnostics.* Report CTH–RF–54, JET–JE4–9002, Göteborg (1985)

[4] K. Drozdowicz: *Remote Control of LeCroy HV4032/2132 High Voltage System.* Report: CTH–RF–61, Göteborg (1988)

[5] R. Cherubini, G. Moschini, R. Nino, R. Policroniades and A. Varela: *Gamma Calibration of Organic Scintillators.* Nucl. Instr. and Meth. **A281** (1989) 349

[6] R. Madey, F.M. Waterman, A.R. Baldwin, J.N. Knudson, J.D. Carlson and J. Rapaport: *The Response of NE-228A, NE-228, NE-224 and NE-102 Scintillators to Protons from 2.43 to 19.55 MeV.* Nucl. Instr. and Meth. **151** (1978) 445